Detection of Epileptic Seizures using Statistical Features in the EMD Domain

by

S M SHAFIUL ALAM

MASTER OF SCIENCE IN ELECTRICAL AND ELECTRONIC ENGINEERING

Department of Electrical and Electronic Engineering

BANGLADESH UNIVERSITY OF ENGINEERING AND TECHNOLOGY

July, 2011

The thesis entitled "**Detection of Epileptic Seizures using Statistical Features in the EMD Domain**" submitted by S M Shafiul Alam, Roll No: 0409062207, Session: April, 2009 has been accepted as satisfactory in partial fulfillment of the requirements for the degree of **Master of Science in Electrical and Electronic Engineering** on July 23, 2011.

BOARD OF EXAMINERS

1. _____ **Chairman**
   Dr. Mohammed Imamul Hassan Bhuiyan (Supervisor)
   Associate Professor
   Department of Electrical and Electronic Engineering
   Bangladesh University of Engineering and Technology
   Dhaka – 1000.

2. _____ **Member**
   Dr. Md. Saifur Rahman (Ex-officio)
   Professor and Head
   Department of Electrical and Electronic Engineering
   Bangladesh University of Engineering and Technology
   Dhaka – 1000.

3. _____ **Member**
   Dr. Mohammad Ariful Haque
   Assistant Professor
   Department of Electrical and Electronic Engineering
   Bangladesh University of Engineering and Technology
   Dhaka – 1000.

4. _____ **Member**
   Dr. Mohammad Rakibul Islam (External)
   Associate Professor
   Department of Electrical and Electronic Engineering
   Islamic University of Technology
   Board Bazar,Gazipur-1704.

CANDIDATE'S DECLARATION

It is hereby declared that this thesis or any part of it has not been submitted elsewhere for the award of any degree or diploma.

Signature of the Candidate

_____

S M Shafiul Alam

DEDICATION

To my beloved wife

TABLE OF CONTENTS

LIST OF FIGURES

LIST OF TABLES

LIST OF ABBREVIATIONS

Acc	Accuracy
ANN	Artificial Neural Network
ANOVA	Analysis of Variance
ApEn	Approximate Entropy
CD	Correlation Dimension
DWT	Discrete Wavelet Transform
ECOC	Error Correcting Output Code
EEG	Electro-encephalogram
EMD	Empirical Mode Decomposition
FD	Fractal Dimension
FFT	Fast Fourier Transform
FN	False Negative
FP	False Positive
IMF	Intrinsic Mode Function
KLD	Kullback-Leibler Divergence
KS	Kolmogorov- Smirnov statistics
LDA	Linear Discriminant Analysis
LLE	Largest Lyapunov Exponent
LOF	Left Orbitofrontal cortex
LST	Left Subtemporal Cortex
LTD	Left Temporal Lobe
MLE	Maximum Likelihood Estimate
MLPNN	Multi-layer Perceptron Neural Network
MSE	Mean Square Error
NIG	Normal Inverse Gaussian distribution
PCA	Principal Component Analysis
pdf	Probability density function
PNN	Probabilistic Neural Network
PSP	Postsynaptic Potential
RBFSVM	Radial Basis Function SVM
RI	Reduced Interference

RNN	Recurrent Neural Network
ROF	Right Orbitofrontal cortex
RST	Right Subtemporal Cortex
RTD	Right Temporal Lobe
SD	Standard Deviation
Sen	Sensitivity
Spec	Specificity
SPWV	Smoothed Pseudo-Wigner-Ville distribution
STFT	Short Time Fourier Transform
SVM	Support Vector Machine
TFA	Time Frequency Analysis
TN	True Negative
TP	True Positive

ACKNOWLEDGEMENT

First and foremost, I would like to express the deepest gratitude to Almighty Allah for blessing me with the physical and mental strength to make a successful completion of the research work.

I express my heartfelt thanks and sincere gratitude to Dr. Mohammed Imamul Hassan Bhuiyan for his kind supervision, patient guidance, and constant support in completing the research work presented in this dissertation. Without his valuable suggestions in various aspects, the successful completion of this thesis wouldn't have been possible. It was an honor for me to be one of his supervisees.

I would also like to thank Prof. Dr. Md. Saifur Rahman, Head of the Department, for sharing some of his precious time in reviewing my thesis work and giving valuable suggestions. My special thanks to Dr. Mohammad Ariful Haque and Dr. Mohammad Rakibul Islam for their kind consent and comprehensive evaluation of the thesis.

And last but not the least; my heartiest thanks are for my wife. Without her mental support and help, it was not possible to make the completion of this dissertation a success.

ABSTRACT

Epilepsy is one of the most common and serious neurological disorders that affects a significant amount of people around the world. It is characterized by sudden occurrence of massive seizure attack, which is unpredictable in nature. The treatment of epilepsy is often carried out through continuous monitoring of the patient using electro-encephalogram (EEG) signals. Since the EEG records are generally of long duration and the number of patients is huge, an automatic system for diagnosis of epilepsy and detection is necessary. In addition, it may aid in focal drug delivery and generating alarm through an implantable device.

Various methods are available in the literature for automatic seizure detection from EEG signals. The most promising performances are reported by those using time-frequency transform domain techniques. Recently, the empirical mode decomposition (EMD) has emerged as a simple and effective method for the analysis of time-series data. Unlike time-frequency transforms, the EMD is data adaptive, not requiring any basis function or assumption in regard to data linearity and stationarity. This is particularly important given that the EEG signals are highly nonlinear and non-stationary. However, limited amount of work is available in the literature that use the EMD analyzing EEG signals to classify them for epilepsy diagnosis and seizure detection.

In this thesis, efficient EMD-based methods are developed classification of EEG signal for subsequent diagnosis of epilepsy and seizure detection. A comprehensive database of EEG records, publicly available online is used for analyzed using statistical and chaotic features extracted from the decomposed intrinsic mode functions. The ability of these features in discriminating the EEG signals is extensively studied. Classification systems are then developed using the statistical and chaotic features in an artificial neural network (ANN). The performance of these classification systems is investigated in terms of sensitivity, specificity and accuracy for various problems of classification regarding real-life medical scenario of epilepsy diagnosis and detection of seizure activity. The results show that the features extracted in EMD domain can classify the EEGs with 100% sensitivity, 100% specificity and 100% accuracy in most of the cases, while requiring reduced computational cost and fewer features. It is further observed that the statistical features play the major role in improving the overall performance compared to the chaotic ones. Finally, an extensive study is conducted to determine whether statistical priors can capture the underlying statistics of EEG signals.

CHAPTER 1

INTRODUCTION

The human brain contains approximately 100 billion neurons or nerve cells. These are involved in the brain's fundamental functions; fast, organized information processing and communication. The neurons transmit information and communicate with each other using a combination of chemical and electrical signals. They are interconnected using *axons* and *dendrites* – analogous to a transmitter and a receiver, respectively (Fig. 1.1(a)).

When the aggregate input to neuron exceeds a threshold value, an action potential occurs and at the axon terminal, it results in the release of neurotransmitter from the pre-synaptic membrane, causing *postsynaptic potentials* (PSP).This is illustrated in Fig. 1.1(b). The black arrow shows an action potential terminating at a synapse. Neurotransmitters are released, causing a PSP with the gray arrow showing an approximation of the macroscopic current.

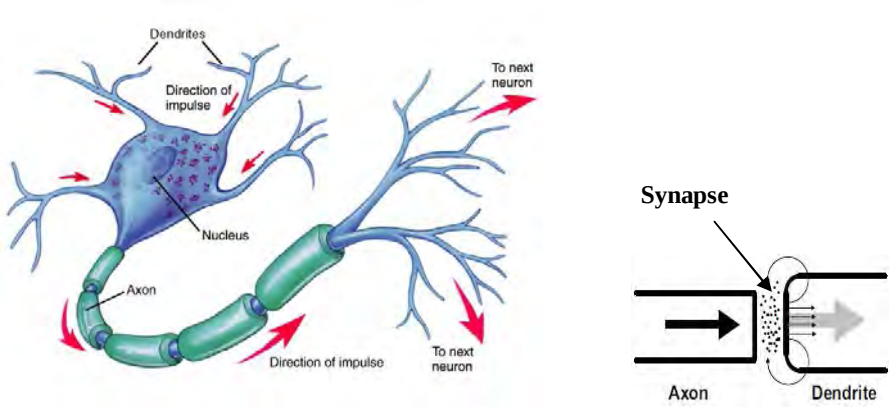

(a) (b)

Fig. 1.1: Transmission of electric signal through a single neuron.

The PSP can be described by a *current dipole*, giving rise to currents in the surrounding tissues, which can exist for several tens of milliseconds causing the so called *volume currents*. For a large group of neurons these volume currents can induce measurable electric and magnetic fields over the cerebral cortex which can be detected using appropriate electric and electro-magnetic transducer. Fig. 1.2 illustrates typical neural activity inside human brain which, can be analyzed by detecting the electro-magnetic effect caused by the activity itself.

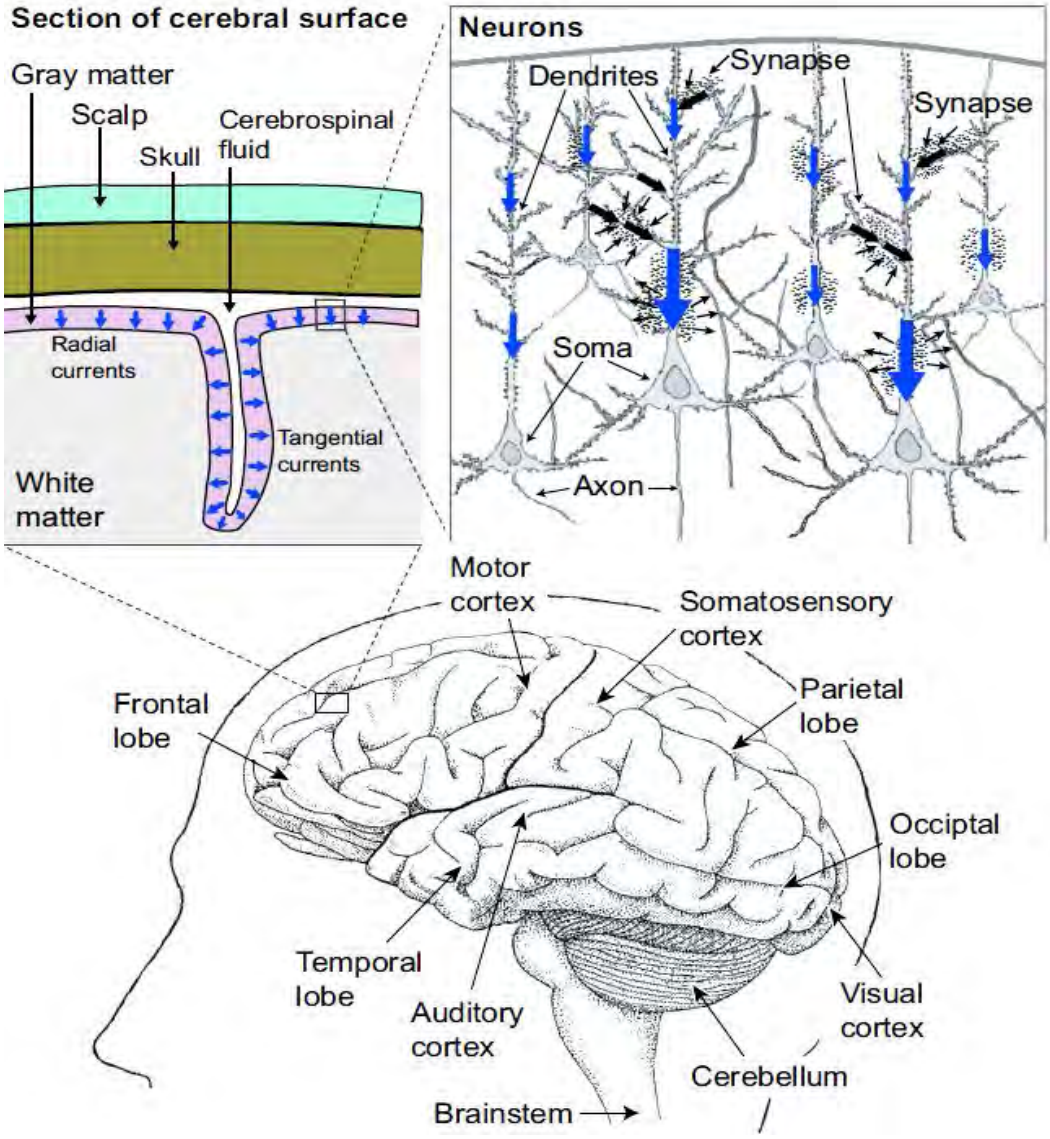

Fig. 1.2: Human brain electrical activity. (Adapted from [1])

1.1 EEG

EEG is the abbreviation of *electroencephalogram* – the name given by a German psychiatrist Hans Berger, who made the first recording of human brain electrical activity in 1924 [2]. EEG recordings are achieved by placing silver-chloride covered electrodes of high conductivity (impedance <5000 Ω) in different locations of the head (scalp EEG). EEG is the measurement of the electric field induced by the neural activity inside the brain. Internationally standardized *10-20 system* is usually employed for electrode placement (Fig. 1.3). In this system 21 electrodes are located on the surface of

the scalp. The positions are determined as follows: Reference points are *nasion*, which is the delve at the top of the nose, level with the eyes; and *inion*, which is the bony lump at the base of the skull on the midline at the back of the head. From these points, the skull perimeters are measured in the transverse and median planes. Electrode locations are determined by dividing these perimeters into 10% and 20% intervals. Three other electrodes are placed on each side equidistant from the neighboring points [3, 4].

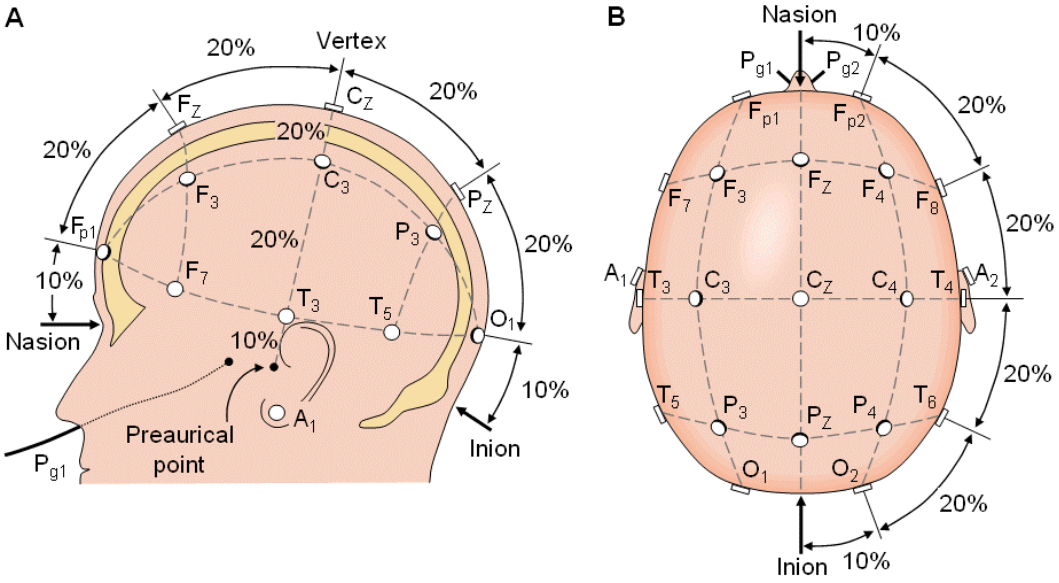

Fig. 1.3: The international 10-20 system seen from (A) left and (B) above the head. A-Ear lobe, C-central, F-frontal, Fp-frontal polar, P-parietal, Pg-nasopharyngeal, O-occipital.

Measures of the electric potentials can be recorded between pairs of active electrodes (*bipolar recordings*) or with respect to a *reference* electrode (*monopolar recordings*). The scalp EEG signals as sensed by the electrodes are generally passed to a multi-channel amplifier system through a protection circuit (Fig. 1.4). The amplified signals are then converted into digital format and are recorded using a computerized data acquisition system. However, a practical EEG recording system is more sophisticated to deal with various artifacts that occur in real life.

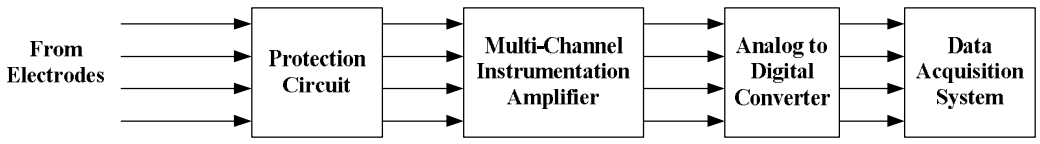

Fig. 1.4: Generalized block diagram of EEG recording system.

The amplitude and frequency content of EEG signals recorded depends on the electrode position as well as both physical and mental states of a person undergoing the process. Generally, the frequency contents of EEG signals are defined according to five sub-bands:

1. δ (0~4 Hz): EEG signals in this frequency range are detectable in infants and sleeping adults.
2. θ (4~8 Hz): The EEG signals of this band are obtained from children and sleeping adults.
3. α (8~12 Hz): EEGs of this frequency range can be measured from the occipital regions (O_1 and O_2 electrode in Fig. 1.3) of an awaken person closed eyes.
4. β (13~30 Hz): EEG signals having this frequency band are detectable over the parietal and frontal lobes (Fig. 1.3).
5. γ (30~60 Hz): The regions of high EEG signals having this highest level of subband are located in the frontocentral area.

Since its first recordings, EEG is used in neuroscience to analyze various neural activities (e.g. sleep stages, sensory and motor activity, emotional state etc.) as well as to diagnose diseases and disorders such as epilepsy, sleep apnea, schizophrenia. Among various neurological disorders, epilepsy is the most common and serious one. About 50 million people world-wide are suffering from epilepsy and 85% of those live in developing countries. Each year 2.4 million new cases are estimated to occur globally [5]. In most of the adult patients, epilepsy occurs in the mesial temporal structures such as hippocampus, amygdala, and parahippocampal gyrus [6]. Epilepsy is characterized by recurrent seizures i.e. physical reactions to sudden, usually brief, excessive electrical discharges in a group of brain cells. Symptoms of a seizure can range from sudden, violent shaking and total loss of consciousness to muscle twitching or slight shaking of a limb. Staring into space, altered vision, and difficult speech are some of the other behaviors that a person may exhibit while having a seizure. The unpredictable nature of seizures is responsible for the enhanced risk of sudden unexpected injury or death. The occurrence of seizure manifests itself by making drastic changes in EEG patterns (Fig. 1.5). The following figure shows typical EEG patterns of an epileptic patient before, during and after the seizure attack. Note that, the EEG patterns are somewhat *spiky* during the occurrence of seizure.

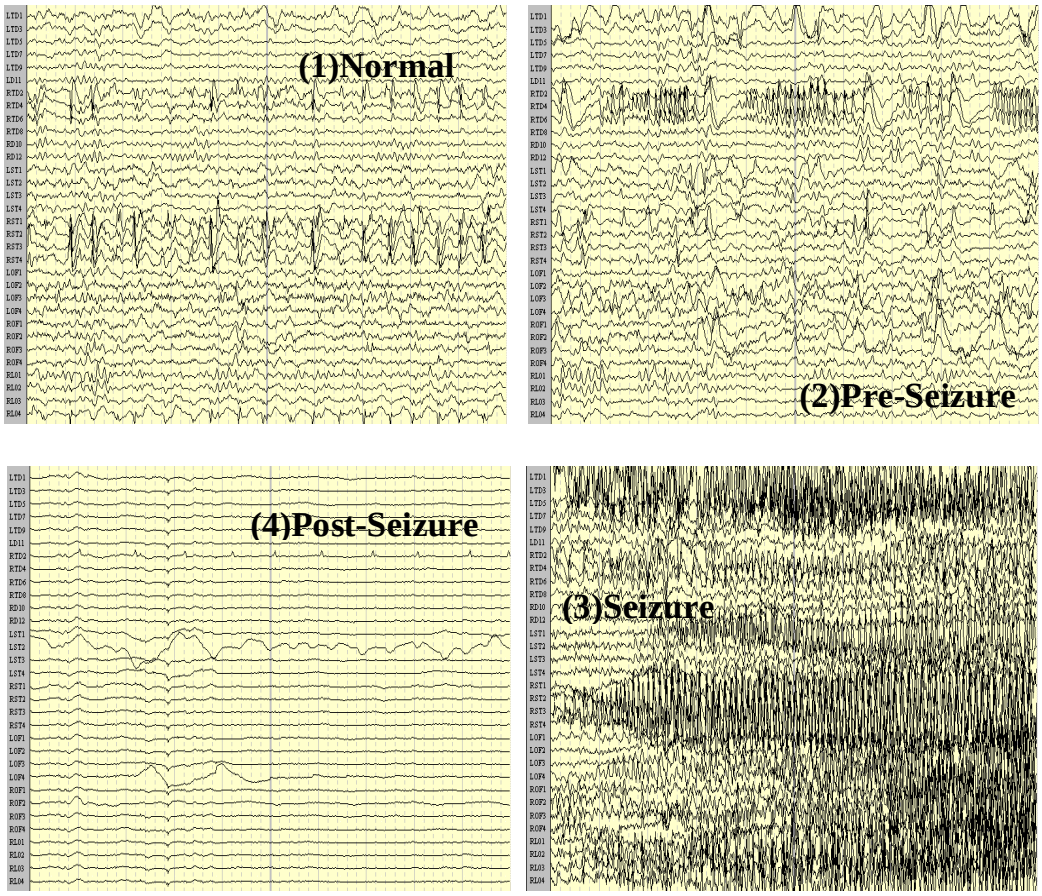

Fig. 1.5: Multi-channel EEG records illustrating the occurrence of seizure.

In general, epilepsy affects the human brain in different locations, defined as *epileptogenic zone* and it may be necessary to monitor the seizure activity more accurately depending on the patient's condition. In these cases, special *intracranial* electrodes are surgically inserted into this zone to record EEG. Fig. 1.6 below shows an example of such electrode placement.

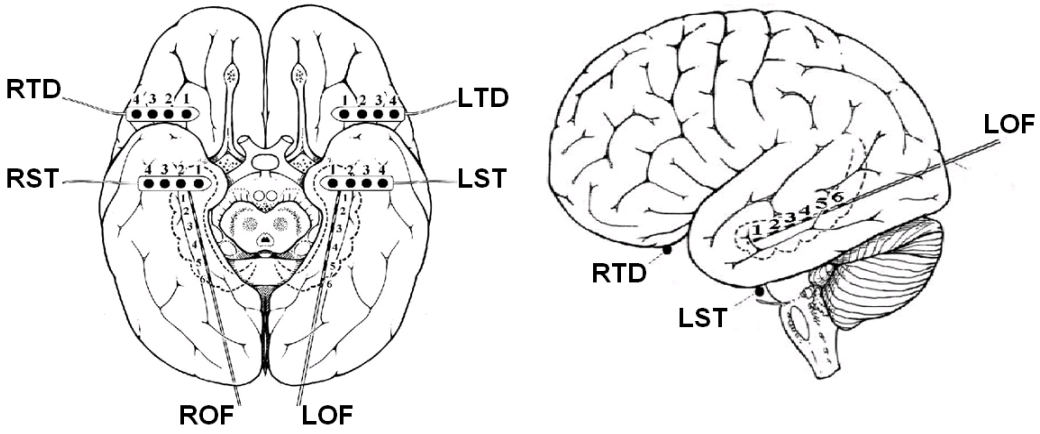

Bottom view Left-side view

Fig. 1.6: Intracranial electrode placement. (Adapted from [7])

As shown on the figure, depth electrodes are inserted at the left and right temporal lobes (LTD, RTD) and subdural electrode strips are symmetrically placed over the orbitofrontal (LOF, ROF) and subtemporal (LST, RST) cortex. The EEG patterns obtained from an epileptic patient are defined as *ictal* and *interictal* that correspond to the condition of non-seizure and seizure attack respectively.

1.2 Motivation

Detection of a seizure attack is traditionally carried out by viewing EEG records of long duration that may even last for several days. Considering the length of the records to be observed and the huge volume of patients, it is often difficult and time consuming for an expert neurologist to locate a seizure. An automatic seizure detection system can considerably reduce the volume of data to be observed. It is to be noted that such a system needs to be highly sensitive, even though that may generate lots of false alarms, since the neurologist could easily discard them. In addition, such a system can be integrated into an implantable device for detecting the onset of seizures and henceforth,

triggers an alarm as well as initiate drug delivery. This is important since often the patient is not in a state to push the alarm and focal drug delivery might be more effective with reduced side effects related to antiepileptic drugs [18].

Various algorithms have been introduced for detecting seizure from EEG records [8 – 22]. Most of these researches are carried out based on the analysis of dynamic behavior of EEG records in inte-rictal and ictal regions. For a time series like EEG, portrait of the reconstructed phase space can be useful in representing EEG dynamics. In [8], a probabilistic analysis is carried out to statistically quantify the changes of points within the reconstructed phase space portrait during seizure and non-seizure activity. For comparison, variance based analysis is also carried out and it is reported that the statistical significance of the two analysis is almost same in distinguishing seizure and non-seizure activities. However, the accuracy level of detecting seizures using these two analyses is not reported. Variance among a set of delay vectors is used in [9]. The set consists of the delay vectors that are within a certain standardized distance. Over a range of this distance, a number of set is defined and corresponding variance is calculated for EEG records of different category. It is observed that the average values of these variances for each category give specific pattern against certain range of standardized distance which is clearly distinguishable. Based on this analysis, nearest neighbor and leave-one-out approach is employed to classify EEG signals into *healthy*, *inteictal* and *ictal* types and their accuracy is reported. In [10], arbitrary thresholding of EEG signal variance is used. Considering the non-stationarity, EEG signals are windowed in small blocks and variance is calculated for each of them. Fixed thresholding is used over these variances to classify the EEG segments into *healthy* and interictal and *ictal* ones. Although, maximum accuracy of classification is reported based on an specific online EEG database, no indication is given about a generalized process (if any) of defining the level of fixed threshold.

Besides, research works in non-linear analysis of the EEG signals using chaos theory are reported in the literature. The general theme of these works is that the dynamic behavior of EEG signals varies in terms of complexity and chaos from a healthy person to an epileptic patient. Chaos is defined as an apparent disorder of a system, highly

sensitive to differences in initial conditions. A number of measures are reported in literature to quantify the level of chaoticity and complexity [8]. In [11], EEG signals are decomposed into five sub-bands using discrete wavelet transform (DWT) and two chaotic features: largest Lyapunov exponent (LLE) and correlation dimension (CD) are obtained from these subbands. These two quantities define the chaoticity and complexity of a dynamic system, respectively. A one-way analysis of variance (ANOVA) shows significant statistical difference among *healthy*, *interictal* and *ictal* segment using these two measures in wavelet subbands. However, no extensive analysis is reported to observe the accuracy of these measures in classifying EEGs into the three mentioned categories in DWT domain. In [12], Lyapunov spectra are used to make three-way (*healthy*, *interictal* and *ictal*) classification employing recurrent neural network (RNN) as the classifier. From the spectra, maximum, minimum, mean and standard deviation (SD) of Lyapunov exponents are used as features. Using similar features obtained from Lyapunov spectra of original EEG time series as well as the wavelet coefficients, a multi-way classification system is reported in [13]. The wavelet coefficients are obtained from the EEG signals using 5-level DWT. These features are fed to a multi-class classifier which is designed from several support vector machines (SVM) employing ECOC (error correcting output code) approach. The performance of this classifier is then compared with that of probabilistic neural network (PNN) and multi-layer perceptron neural network (MLPNN) for the same feature set. In [14], two sets of features are used to deal with a number of classification problems relevant to practical scenario of epilepsy diagnosis and seizure detection. One feature set consists of the estimated parameters of autoregressive model of EEG signals. The EEG signals are then divided into several sub-windows and power spectral analysis is carried for each of them using fast Fourier transform (FFT). The power spectra are divided into fifteen sub-bands and their mean energies are used to constitute another feature set. In addition to that, approximate entropy (ApEn), a thermodynamic quantity defining system regularity or randomness is calculated for each sub-window, which is also included in both sets of features. A comprehensive study is carried out by feeding these two feature sets to various linear and non-linear classifiers and effect of window size, feature reductions is reported. In [15], Fractal dimension (FD) is used as feature in classifying *healthy* and *ictal* EEG segments employing SVM. A comparative study is reported showing the effect of choosing different kernels for SVM as well as different

algorithm to calculate FD. In [16], ApEn and linear statistical measures such as variance, skewness and kurtosis obtained from the EEG signals are utilized as features and fed to a linear classifier to distinguish normal and seizure activities. Later, Fisher's Discreminant analysis is used in [17] to make optimum selection of features from four linear statistical measures such as variance, skewness, kurtosis and coefficient of variance to obtain the highest accuracy in classifying *healthy* and *ictal* EEG segments. It should be noted that, the analyses reported in [15 – 17] consider the problem of classification resembling *epilepsy diagnosis*. No performance is reported about classifying *interictal* and *ictal* EEGs, relevant to *seizure detection*. In medical perspective, detection of seizure is not less important than the diagnosis of epilepsy and thus can't be considered unnoticed.

As mentioned earlier, occurrence of seizure activity manifests itself by drastic change and giving a *spiky* wave patterns in EEG signals. Such an EEG record if decomposed into the five sub-bands ($\delta - \gamma$) can show how seizure affects the response of EEG in different sub-bands. Due to non-stationary nature, the frequency response is time-varying and for this reasons a composite analysis in both time and frequency domain is necessary for EEG signals to observe the effect of seizure and non-seizure activities. Application of time-frequency analysis (TFA) in classifying different EEGs is reported in [18, 19]. Smoothed pseudo-Wigner-Ville (SPWV) distribution is used in [18] to analyze EEG signals in time-frequency domain. The time span is divided into different number of partitions and the frequency range is divided into different number of sub-bands. Time-frequency grid is thus obtained for each combination of frequency sub-band and time partitions. Energy of each time-frequency gird is used as features. These features are fed to a feed-forward artificial neural network (ANN) in order to classify the EEGs in various categories. Four classification problems are studied for different combinations of time windows and frequency sub-bands. The performance of classification is reported for each combination of time-frequency grid. Further extensive analysis is carried out in [19] for a number of time-frequency distributions such as short time Fourier transform (STFT), SPVW, reduced interference (RI) etc. In this case, three time windows and five frequency sub-bands are used for all time-frequency distributions. A comparative study of ANN based classification shows that the best performance for all classification problems is achieved when RI and SPVW are used for

TFA of EEG signals. Although, TFA can give high degree of accuracy, its computational complexity should also be considered to meet the objective of a fast and efficient practical seizure detection system.

Recently, the empirical mode decomposition (EMD) has drawn the attention of researchers in nonlinear signal analysis for being intuitive and adaptive to signals, while requiring no assumption in regard to stationarity and linearity [20]. Since the EEG signals exhibit non-stationary behavior, a number of methods have been developed to detect seizures in the EMD domain. The EMD can decompose a signal in to a number of distinct oscillatory modes called intrinsic mode function (IMF). In [20], EEG signal is empirically decomposed into IMFs and then the mean frequencies are obtained from the Fourier-Bessel expansion series of these IMFs. These mean values are shown to be effective in discriminating the ictal periods from the inter-ictal ones. However, the applicability of these mean frequencies is not evaluated by considering a classification problem related either to epilepsy diagnosis or seizure detection. Energy thresholding for the first three IMFs are used in [21] to identify inter-ictal and ictal segments from EEG records of epileptic patients. The threshold level for an IMF is defined from its own energy content and the detection of seizure activity is based on whether the three IMF energies exceed their respective threshold levels for certain duration. Power spectral densities of the first three IMFs are used in [22], to extract several statistical features both in time and frequency domain. The dimension of the feature vectors are reduced using Lambda of Wilks criterion and then applied to a linear discriminant analyzer (LDA) for detecting inter-ictal and ictal segments from EEG records of an epileptic patient.

It should be noted that the works of [21-22] do not conduct any comprehensive analysis of EEG signals in the EMD domain and consider only the classification of signals collected during ictal and inter-ictal periods, neglecting the other classifications related to medical applications (e.g., diagnosis of epilepsy) In fact, very limited work is done to analyze different classification problems using features obtained from IMFs of EEG signal. Thus, it might be worthwhile to explore the potential of EMD for EEG signal analysis comprehensively and develop classification systems suited to a variety of classification problems.

1.3 Objective and Scope

The objective of this thesis is to develop effective classification methods with improved accuracy for use in epilepsy diagnosis as well as detecting seizure activity. The efficacy of a classification system depends mostly on the types of the features used and whether they are extracted from original or transformed signals. In this regard, a comprehensive analysis of EEG signals will be done in the EMD domain to investigate the effectiveness of higher order statistical features such as variance, kurtosis and skewness in discriminating EEG segments of different characteristics. An ANN based classification system shall be developed using these statistical features and its performance studied for different classification problems extensively. Furthermore, the possibility of EEG signal discrimination using chaotic features will be explored. An extensive study will be conducted to determine the potentiality of chaotic features extracted in the EMD domain in discriminating the EEG signals. A classification system will then be developed using a combination of the statistical and chaotic features and its performance investigated for different classification problems. Since the variance, kurtosis and skewness provide an average characterization of different order EEG signals, it might more interesting to see whether the statistics of these signals can be effectively described using statistical models. This is important as given that a model capture the underlying statistics of an EEG signal, whether in time or EMD domain, the corresponding model parameters may provide valuable information as to the signal characteristics related to epilepsy. Thus, the performance of a number of well-known statistical priors in describing the underlined statistics of original EEG signals as well as the decomposed IMFs will be investigated.

1.4 Organization

The thesis is organized as follows. In Chapter 2, the suitability of kurtosis, skewness and variance in classifying EEG signals is investigated in the EMD domain. The performance of the ANN-based classification method, wherein these features are used as patterns, is described for various classification problems related to medical scenario involving epilepsy diagnosis and seizure detection. In Chapter 3, chaotic analysis is carried out on the IMFs to observe their capability of distinguishing various types of EEG signals. Performance of the classification method employing a combination of statistical and chaotic features of the IMFs is described in Chapter 4. In Chapter 5, EEG signals are modeled using various statistical priors and the performance of these priors in modeling the signals is described using standard measures of goodness-of-fit. Finally, in Chapter 6, the research work presented in this thesis is summarized and recommendation for future research is stated.

CHAPTER 2

DETECTION OF EPILEPTIC SEIZURES USING HIGHER-ORDER STATISTICS IN THE EMD DOMAIN

2.1 Overview

In this chapter, a method for efficient detection of seizure using higher order statistical moments calculated in the EMD domain is proposed [23]. The suitability of these moments in distinguishing the EEG signals is investigated through an extensive analysis in the EMD domain. An artificial neural network (ANN) is employed as the classifier of the EEG signals wherein these moments are used as features. The performance of the proposed method is studied using a publicly available comprehensive database for various classification categories and compared with that of several recent techniques. It is shown that the proposed method can provide very high degree of sensitivity, specificity and accuracy especially in the case of discriminating seizure activities from the non-seizure ones for patients with epilepsy.

2.2 Empirical Mode Decomposition (EMD)

The EMD is an adaptive process of extracting amplitude and frequency modulated oscillatory patterns directly from a time series data. The decomposition is based on the simple assumption that any data consists of different simple intrinsic modes of oscillations which can be extracted using the basis derived from the data. These patterns are called intrinsic mode functions (IMFs) and they satisfy the following two conditions [24]:

a) For an IMF, total number of maxima and minima equals to the total number of zero crossings or differs at most by one.

b) At any point of the IMF, the mean value of the envelope defined by the local maxima and the envelope defined by the local minima is zero.

The process of extracting IMFs from a time series data is called a *Sifting* process. It should be noted that, the signal should have at least one maxima and on minima for successful decomposition. For an N-point data, $X\{x_1, x_2, ..., x_N\}$, the sifting process is carried out as follows:

Step 1: The original data (X) is assigned to an initial dummy variable, h

$$h=X \tag{2.1}$$

Step 2: h assigned to another variable, h_{old}

$$h_{old} = h \tag{2.2}$$

Step 3: The local maxima and minima of h_{old} are identified. The j^{th} sample of h_{old} is considered to be local maxima if it is greater than both the $(j+1)^{th}$ and $(j-1)^{th}$ sample and minima if it is less than both the $(j+1)^{th}$ and $(j-1)^{th}$ sample.

Step 4: Envelops of local maxima e_{max} and that of local minima e_{min} are obtained using the following method of *cubic spline interpolation.*

The interpolation is based on defining a set of piece-wise 3rd degree polynomials, *F(z)* for *P*-point data $\{z_1, z_2, \ldots z_P\}$

$$F(z) = f_i(z);\ z_i \le z < z_{i+1};\ i = 1, 2, 3, \ldots, P-1; \tag{2.3}$$

where, $f_i(z) = a_i(z-z_i)^3 + b_i(z-z_i)^2 + c_i(z-z_i) + d_i$ and z denotes the set of either the local maxima or the local minima. The parameters a_i, b_i, c_i and d_i are estimated as:

$$a_i = \frac{M_{i+1} - M_i}{6(z - z_i)};\ b_i = \frac{M_i}{2};\ c_i = \frac{y_{i+1} - y_i}{(z - z_i)} - \left(\frac{M_{i+1} + 2M_i}{6}\right)(z - z_i) \text{ and } d_i = y_i$$

for $y_i = F(z_i)$ and $M_i = f_i''(z_i)$

Step 5: The values of the mean of e_{max} and e_{min} are calculated

$$M = (e_{max} + e_{min})/2 \tag{2.4}$$

and subsequently subtracted from h_{old}

$$h_{new} = h_{old} - m \tag{2.5}$$

Step 6: h_{new} is then assigned to h_{old}

$$h_{old} = h_{new} \tag{2.6}$$

Steps 3 – 6 are repeated until the following stopping criterion is fulfilled.

$$SD = \frac{\sum |h_{new} - h_{old}|^2}{\sum h_{old}^2} < \alpha \tag{2.7}$$

where α is an arbitrary value preset in the range of 0.2~0.3. Upon satisfying eqn. (2.7), h_{new} becomes an IMF *c*, a residue value *r* is calculated as

$$r = h - c \tag{2.8}$$

The entire process is then repeated by setting *r* as *h*. Thus, the input signal can be decomposed into *L* IMFs until the residue becomes a monotonic function such that further extraction of an IMF is not possible. Fig. 2.1 illustrates the whole process using a flow chart.

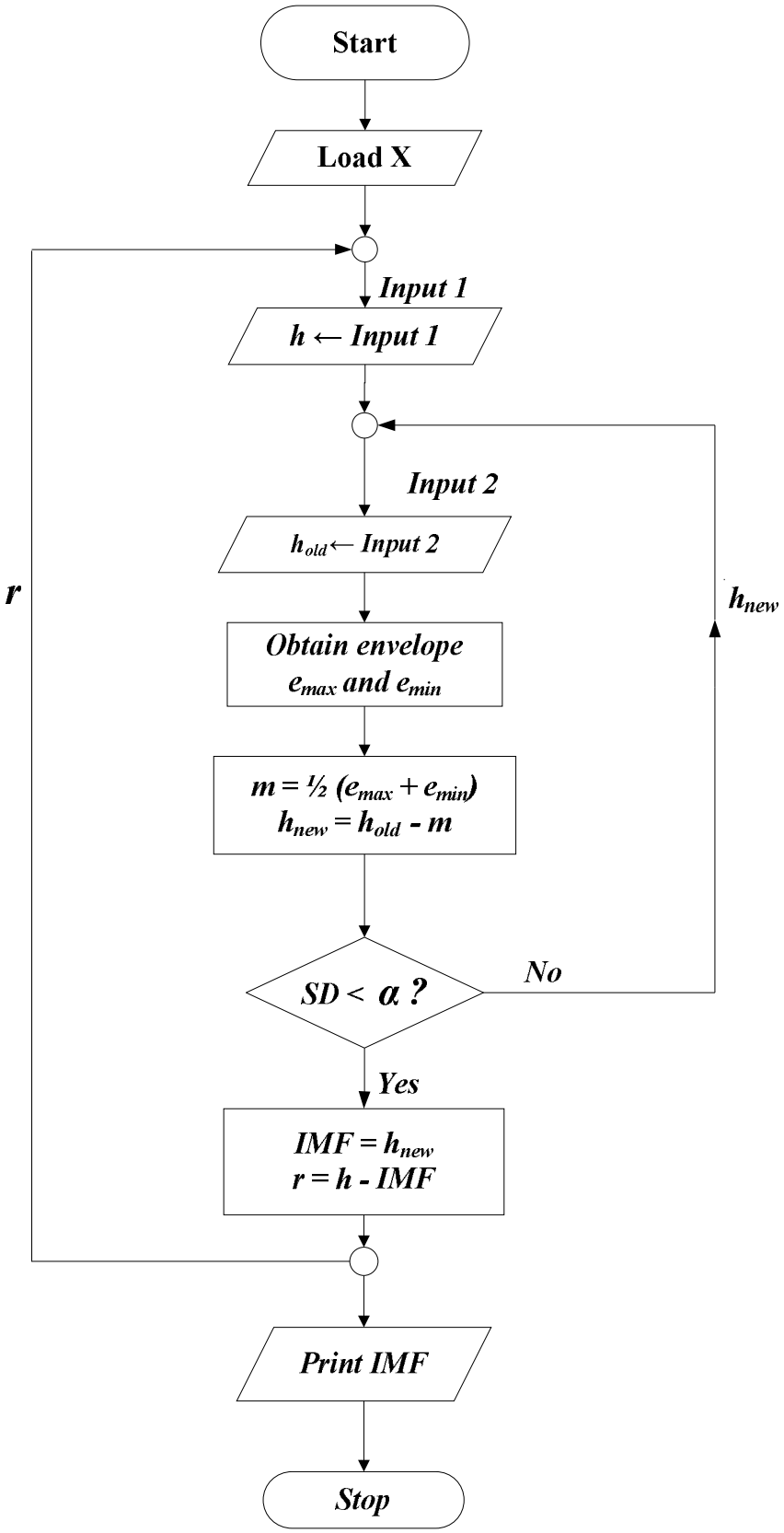

Fig. 2.1: Flow Chart describing EMD.

The input X can be reconstructed from all the IMFs as

$$X = \sum_{n=1}^{L} c_n + r_L \tag{2.9}$$

As mentioned in Sec. 1.5, EMD is particularly well-suited for analysing non-stationary and non-linear signals and further investigations is required to evaluate its applicability in EEG signal analysis. As a first attempt, an original EEG segment and its first four empirically decomposed IMFs are shown on Fig. 2.2. Notice that as the level of an IMF increases, the corresponding data becomes smoother.

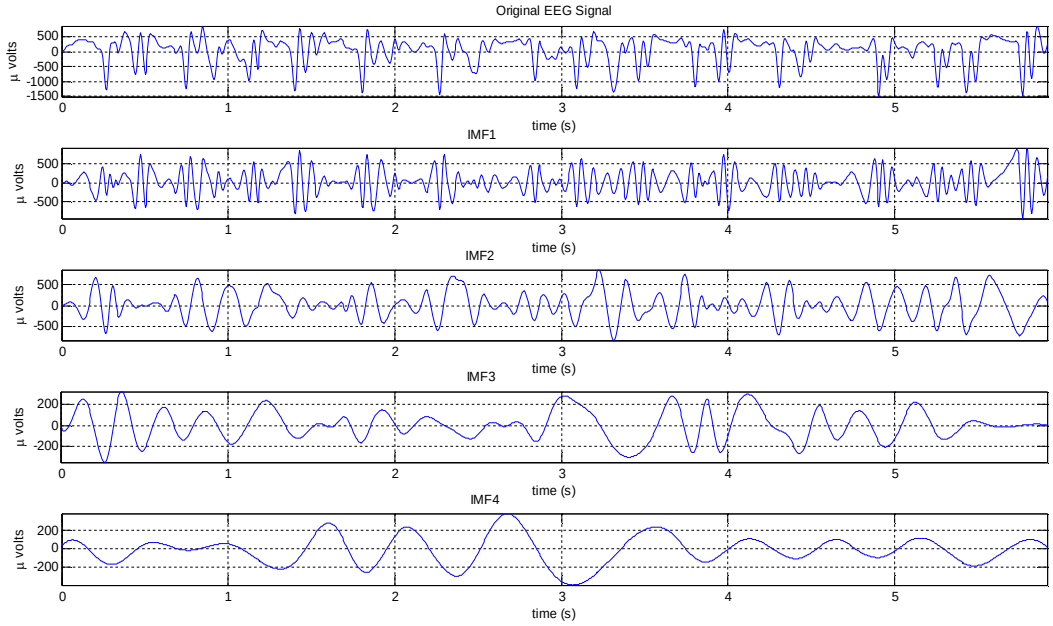

Fig. 2.2: Sample EEG signal and its first four IMFs.

2.3 Analysis of EEG Signals Using Higher Order Statistics

In this work, higher order statistics such as variance, skewness and kurtosis are utilized for classifying the EEG signals in the EMD domain. The use of these moments is motivated by the fact that distribution of the samples of a data set is often characterized by its level of dispersion, asymmetry and concentration around the mean. For an N-point data, $X\{x_1, x_2,..., x_N\}$, the variance σ^2 is calculated as

$$\sigma^2 = \frac{1}{N}\sum_{i=1}^{N} (x_i - \mu)^2; \mu = \frac{1}{N}\sum_{i=1}^{N} x_i \tag{2.10}$$

where μ denotes the sample mean of the data. The skewness β_1 is measured as

$$\beta_1 = \frac{1}{N}\sum_{i=1}^{N}\left(\frac{x_i - \mu}{\sigma}\right)^3 \tag{2.11}$$

If skewness is negative, the data are spread out more to the left of the mean than to the right. On the other hand, a positive skewness indicates that the data are spread out more to the right. For a perfectly symmetric distribution about mean, the skewness would be equal to zero. The kurtosis β_2 is obtained as

$$\beta_2 = \frac{1}{N}\sum_{i=1}^{N}\left(\frac{x_i - \mu}{\sigma}\right)^4 \tag{2.12}$$

The kurtosis of a data histogram having a sharper peak and longer, fatter tails is greater than that for a distribution having a more rounded peak and shorter thinner tails. Notice that the variance itself is the 2nd – order moment of the data, whereas the skewness and kurtosis are computed from the 2nd, 3rd and 4th – order moments. Fig. 2.3 shows the plot of histograms of EEG signals obtained from a healthy person and an epileptic patient during inter-ictal and ictal periods.

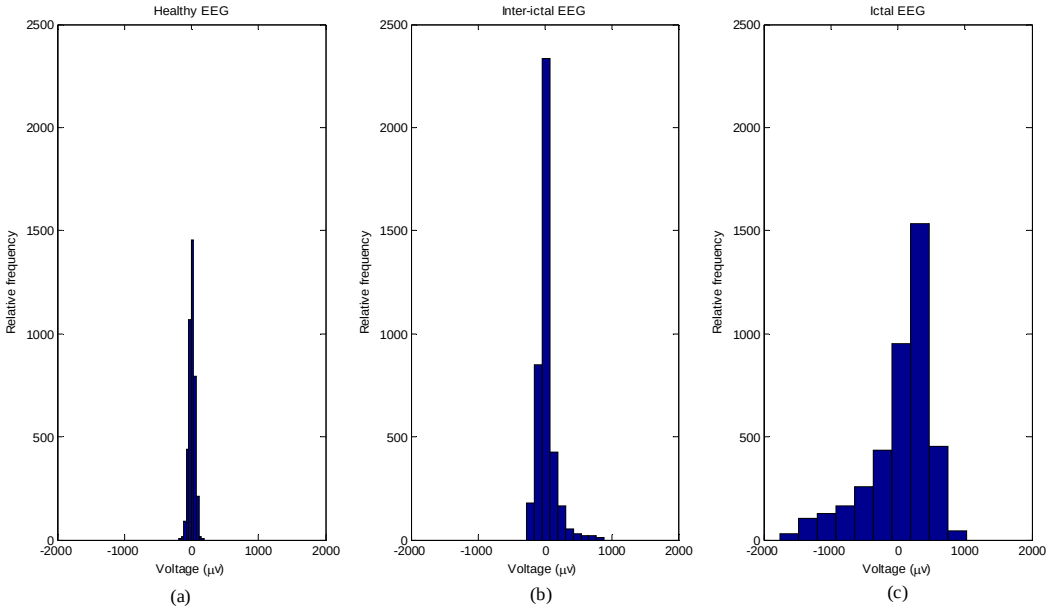

Fig. 2.3: Histograms of (a) healthy, (b) inter-ictal and (c) ictal EEG segment.

It is seen that ictal ones demonstrate the highest level of dispersion, whereas the non-ictal one (healthy) the smallest. However, these two show a similar level of peakedness. On the other hand, the inter-ictal (seizure-free interval) segment gives considerably higher peak. The healthy, inter-ictal and ictal segments are symmetric, asymmetric to the right and asymmetric to the left with respect to the corresponding mean, respectively, the ictal one being more asymmetric than others.

Since the measures, variance, skewness and kurtosis, are representative of the dispersion, asymmetry and peakedness of the data, and hence, may be used to discriminate EEG signals of different categories. However, since the EEG signals are non-stationary, it might be more interesting to see whether similar discriminatory attributes are observed in the EMD domain for these statistical measures. For this purpose, an extensive study is conducted using a comprehensive database of EEG signals, in which the values of these measures are calculated for a large number of EEG segments as well as their various IMFs. The database consists of five hundred EEG segments and is available online [25]. The reason for using the database is its availability in public domain and its widespread use in the literature. It is a collection of 500 single-channel EEG segments of 23.6-sec. duration that are categorized into five groups of 100 segments each (Set A – Set E). Set A and Set B consist of surface EEG segments collected from five healthy volunteers in awaken and relaxed state, with their eyes open and closed, respectively. Segments in Set C, D and E are obtained from five epileptic patients. Set C and Set D contain inter-ictal EEGs recorded intracranially from the hippocampal formation of the opposite hemisphere and the epileptogenic zone of the brain, respectively. Set E contains signals corresponding to seizure attacks (i.e. ictal EEGs). The signals are recorded in digital format at a sampling rate of 173.61Hz omitting the artifacts caused either by muscle activity or strong eye movements [26]. Thus, the sample length of each segment is $173.61 \times 23.6 \approx 4097$, and the corresponding maximum frequency content is 86.81 Hz. Since the frequency range of an EEG signal spans over 0~60 Hz [11], frequencies greater than 60 Hz are considered as noise and discarded by passing each signal through a 6^{th} – order Butterworth filter having a cut-off frequency of 60 Hz. Fig. 2.4 illustrates sample EEG segments from each of these data sets.

For the purpose of analysis, each EEG segment is decomposed into nine IMFs using the algorithm described in Section 2.2. Due to the non-stationary nature, an IMF is further segmented into 16 blocks using a rectangular window of length 256. For each window, the values of the variance, skewness and kurtosis are calculated using (2.10), (2.11) and (2.12). For the sake of comparison, these values are also calculated for the band-limited EEG segments.

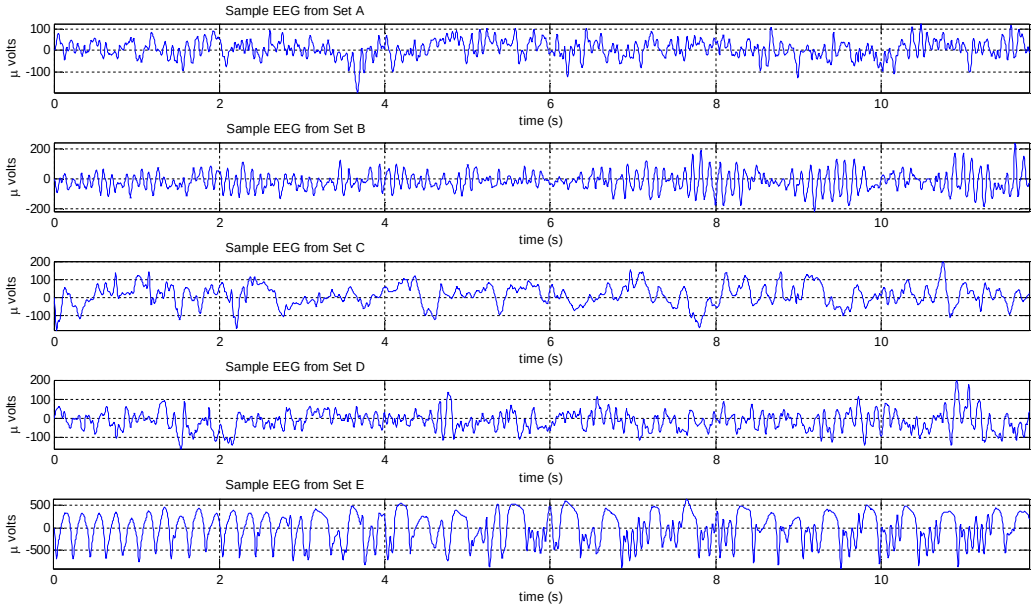

Fig. 2.4: Sample EEG segments from the five datasets.

Tables 2.1, 2.2 and 2.3 shows the mean and standard deviation (SD) of the values obtained for the different sets of EEG signal as well as their IMFs. It can be seen that the mean values are clearly distinguishable for the different sets of EEG signals, especially between the ictal and non-ictal ones. Also, note that the difference becomes larger in the EMD domain as compared to that of band-limited signal. The values of the standard deviation are small for all the parameters except the variance. However, the standard deviations are greatly reduced for the IMFs. In addition, for the set E (that contains signals of ictal period) the mean values of variance are quite large in comparison to those of other sets. It is also seen that the values of variance rapidly decreases with the increase in IMF level.

Table 2.1: Mean values of variance (SD shown in parentheses)

	Set A	**Set B**	**Set C**	**Set D**	**Set E**
Band-limited	1611.324 (815.45)	3953.915 (2913.945)	2845.639 (2611.025)	7299.808 (23242.150)	114858.022 (104905.175)
IMF 1	480.318 (315.588)	2653.632 (2747.498)	292.097 (434.722)	1059.390 (5059.273)	57976.683 (75834.202)
IMF 2	359.685 (212.33)	675.571 (442.931)	625.770 (699.974)	1592.860 (5748.099)	55920.001 (66271.258)
IMF 3	277.509 (225.947)	367.282 (357.469)	894.746 (1170.022)	2054.435 (6744.977)	22487.367 (32335.638)
IMF 4	283.841 (357.366)	326.523 (641.159)	752.704 (1152.976)	1984.115 (7380.363)	9063.732 (18489.421)
IMF 5	215.720 (330.739)	221.450 (493.7)	334.132 (559.707)	1932.679 (12947.829)	2810.065 (7526.228)
IMF 6	90.585 (405.294)	104.666 (302.232)	73.602 (196.305)	897.671 (7431.247)	885.594 (5008.929)
IMF 7	50.696 (244.555)	69.882 (235.147)	35.741 (130.478)	144.141 (1053.630)	273.489 (1871.726)
IMF 8	22.330 (68.212)	51.857 (168.252)	24.766 (98.504)	30.891 (121.214)	89.201 (250.402)
IMF 9	10.658 (31.306)	15.042 (34.457)	8.514 (24.825)	14.666 (61.237)	30.986 (67.602)

Table 2.2: Mean values of skewness (SD shown in parentheses)

	Set A	**Set B**	**Set C**	**Set D**	**Set E**
Band-limited	-0.018 (0.342)	0.032 (0.306)	-0.107 (0.513)	0.055 (0.781)	-0.062 (0.795)
IMF 1	0.002 (0.153)	-0.006 (0.133)	0.013 (0.288)	0.026 (0.393)	-0.012 (0.243)
IMF 2	-0.004 (0.195)	0.004 (0.164)	0.013 (0.260)	0.002 (0.297)	-0.006 (0.187)
IMF 3	0.001 (0.259)	-0.003 (0.284)	0.000 (0.332)	0.015 (0.321)	-0.007 (0.258)
IMF 4	0.007 (0.347)	0.003 (0.368)	-0.016 (0.377)	-0.008 (0.390)	0.003 (0.353)
IMF 5	-0.010 (0.475)	0.004 (0.466)	0.019 (0.484)	0.002 (0.473)	0.008 (0.460)
IMF 6	0.017 (0.645)	0.009 (0.658)	0.010 (0.663)	0.001 (0.647)	-0.002 (0.633)
IMF 7	0.018 (0.626)	0.030 (0.607)	0.027 (0.604)	0.007 (0.597)	0.006 (0.607)
IMF 8	0.006 (0.493)	0.026 (0.486)	0.048 (0.456)	0.024 (0.469)	0.014 (0.490)
IMF 9	0.010 (0.364)	0.042 (0.358)	0.038 (0.312)	0.028 (0.326)	0.021 (0.361)

Table 2.3: Mean values of kurtosis (SD shown in parentheses)

	Set A	**Set B**	**Set C**	**Set D**	**Set E**
Band-limited	2.971 (0.599)	2.949 (0.550)	3.041 (0.940)	3.456 (2.238)	3.237 (1.210)
IMF 1	3.312 (0.912)	3.188 (0.917)	4.017 (1.522)	4.707 (2.337)	3.070 (1.439)
IMF 2	2.871 (0.719)	2.839 (0.707)	3.108 (0.859)	3.271 (1.278)	2.582 (0.826)
IMF 3	2.618 (0.645)	2.586 (0.671)	2.596 (0.729)	2.630 (0.778)	2.451 (0.680)
IMF 4	2.216 (0.563)	2.196 (0.598)	2.147 (0.554)	2.189 (0.610)	2.124 (0.548)
IMF 5	1.928 (0.559)	1.903 (0.567)	1.889 (0.562)	1.891 (0.581)	1.909 (0.512)
IMF 6	2.098 (0.568)	2.132 (0.567)	2.147 (0.549)	2.112 (0.549)	2.089 (0.566)
IMF 7	2.157 (0.527)	2.138 (0.509)	2.136 (0.513)	2.126 (0.512)	2.133 (0.518)
IMF 8	2.025 (0.399)	2.015 (0.378)	1.997 (0.366)	2.006 (0.384)	2.004 (0.450)
IMF 9	1.906 (0.348)	1.923 (0.299)	1.767 (0.547)	1.758 (0.587)	1.868 (0.439)

Next, a one-way analysis of variance (ANOVA) is performed at 99% confidence level to observe the ability of discrimination of a particular measurement over the band-limited EEGs as well as IMFs. Significant statistical difference among the five groups is indicated when $p < 0.001$. Table 2.4 shows the results obtained from the ANOVA.

Table 2.4: *p*-values obtained from one-way ANOVA analysis

Signals	***p*-values for Kurtosis**	***p* -values for Skewness**	***p* -values for Variance**
Band-Limited	**0**	**1.11E-16**	**0**
IMF 1	**0**	**1.96E-04**	**0**
IMF 2	**0**	0.12331204	**0**
IMF 3	**9.53E-14**	0.27357587	**0**
IMF 4	**1.48E-05**	0.38668119	**0**
IMF 5	0.2694423	0.53907444	**0**
IMF 6	0.0208843	0.92752396	**1.11E-15**
IMF 7	0.5289733	0.70355458	**3.26E-13**
IMF 8	0.3048336	0.12701895	**0**
IMF 9	**0**	0.07286216	**0**

It is observed that kurtosis gives significant statistical difference among five groups for band-limited EEGs as well as the first four IMFs. Skewness does the same for band-limited EEGs and IMF1. However, variance gives significant statistical difference for band-limited EEGs as well as for all the IMFs. These observations are concurrent with that of [20] where it is shown that significant statistical difference exist among the first four IMFs.

2.4 Classification

In the previous section, it is seen that the values of the statistical parameters, variance, skewness and kurtosis are significantly different from each other for different classes of EEG signals especially for the first four IMFs. Thus, a classifier is developed using these parameters as features to differentiate various types of EEG signals. The features are obtained from the IMFs as well as band-limited EEG segment using the procedure described in the previous section. Since an EEG segment is divided into 16 blocks and there are 100 segments in a set, 1600 feature vectors of dimension three are constructed a particular set. These feature vectors are fed into an ANN to perform classification process. The ANN used is a two-layer feed-forward neural network (Fig. 2.5), where both the hidden and output layer neurons use hyperbolic tangent sigmoid transfer function of the form [27]

$$y = f(x) = \frac{2}{1+e^{-2x}} - 1 \tag{2.13}$$

The use of such a non-linear transfer function allows the two-layer network learn the non-linear relationship among the input (feature set) and output (target class) vectors. After random initialization, the weight and bias values are tuned, using a back-propagation training algorithm to optimize the network performance by minimizing the mean square error (MSE) among the target and network output vectors. The training algorithm performs necessary computations backward through the network and updates the network weights and biases to the direction toward which, MSE decreases most rapidly.

For the present analysis, the number of neurons is set to 20 in the hidden layer. In the output layer, the number of neurons is set equal to the number of target classes. The scaled conjugate gradient algorithm [28] is used to train the network using the feature vectors. Training stops when MSE tends to increase during the validation process. The training, validation and testing for classification are carried out using the well-known MATLAB® software package, where 60%, 5% and 35% of the feature vectors are selected randomly for the purpose of training, validation and testing, respectively. For the sake of comparison, an independent classifier is developed for each of the band-limited signal and the corresponding first four IMFs. For the five sets of EEG records described earlier, five different cases of classification problem are considered in this paper. In Case I, the EEG records are classified into three categories. EEG segments from Set A and Set B are tagged together as *healthy* class. Set C and Set D are grouped into the *inter-ictal* class and the Set E the *seizure* class. In Case II, Set A, D and E are classified into *healthy*, *inter-ictal* and *seizure* classes, respectively. In Case III, segments from Set A and Set E are classified into *healthy* and *seizure* classes, respectively. In Case IV, Set A, B, C, and D are tagged together to form the *non-seizure* class, whereas Set E the *seizure* class. In Case V, Set D and Set E are classified into the *inter-ictal* and *seizure* classes, respectively. Table 2.5 shows the distribution of the feature vectors randomly chosen for training, validation and testing purposes.

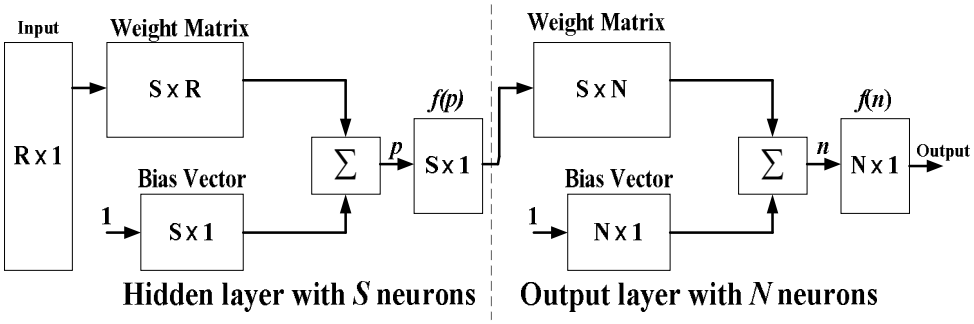

Fig. 2.5: Two layer feed-forward network with *R* input elements and *N* output elements. (Dimension of each matrix / vector is given inside the corresponding blocks.)

Table 2.5: Distribution of the feature vectors

Case	Class	Number of feature vectors randomly chosen			
		Training	**Validation**	**Testing**	**Total**
I	*healthy* (AB)	1920	160	1120	3200
	interictal (CD)	1920	160	1120	3200
	seizure (E)	960	80	560	1600
Total		**4800**	**400**	**2800**	**8000**
II	*healthy* (A)	960	80	560	1600
	interictal (D)	960	80	560	1600
	seizure (E)	960	80	560	1600
Total		**2880**	**240**	**1680**	**4800**
III	*healthy* (A)	960	80	560	1600
	seizure (E)	960	80	560	1600
Total		**1920**	**160**	**1120**	**3200**
IV	*non-seizure* (ABCD)	3840	320	2240	6400
	seizure (E)	960	80	560	1600
Total		**4800**	**400**	**2800**	**8000**
V	*interictal* (D)	960	80	560	1600
	seizure (E)	960	80	560	1600
Total		**1920**	**160**	**1120**	**3200**

2.5 Results and Discussion

The performance of the proposed method is studied using standard measures such as sensitivity (*Sen*), specificity (*Spe*) and accuracy (*Acc*), expressed as

$$Sen = \frac{TP}{TP + FN} \times 100\% \tag{2.13}$$

$$Spec = \frac{TN}{TN + FP} \times 100\% \tag{2.14}$$

$$Acc = \frac{TP + TN}{TP + TN + FP + FN} \times 100\% \tag{2.15}$$

where *TP, TN, FP and FN* stand for true positive, true negative, false positive and false negative events, respectively [14]. The results obtained from the proposed classification algorithm are given in Table 2.6 in terms of sensitivity, specificity and accuracy for the five cases mentioned earlier. Notice that all the cases are closely related to practical medical scenario.

It is seen that the classification performance improves in the EMD domain as compared to that of using the band-limited signals. For Case I, the best result is obtained for IMF 3 where, the sensitivity for *inter-ictal* and *seizure* class are 99.93% and 99%, respectively. This signifies a high degree of accuracy in classifying these two classes of EEG signals.

However, the corresponding sensitivity for the *healthy* class is 50.06%. This result is not unexpected since one can see from Tables 2.2 and 2.3 that the mean values of skewness and kurtosis obtained from IMF 3 are almost same for Set A to Set D. It should be mentioned that an EEG detection method is expected to be highly sensitive especially in the case of *inter-ictal* and *seizure* classes EEG data.

Table 2.6: Classification performance for the various cases

Case		**Band-Limited EEG**	**IMF 1**	**IMF 2**	**IMF 3**	**IMF 4**
I (A,B), (C,D), E	Sen_{AB}	76.81	71.8	50.34	50.06	49.6
	Sen_{CD}	43.23	57.03	**98.4**	**99.93**	**99.22**
	Sen_E	87.88	78.44	82.2	**100**	70.88
Accuracy		65.6	67.2	75.9	80	73.7
II A, D, E	Sen_A	89.8	78	**100**	**100**	1576
	Sen_D	36.75	57.44	**96.56**	**100**	**99.3**
	Sen_E	**94.4**	86	79.5	**100**	63.31
Accuracy		73.6	73.8	92	**100**	87
III A, E	*Sen*	**99.9**	**99.3**	**100**	**100**	**99.9**
	Spec	**98.4**	87.8	**100**	**100**	75.1
Accuracy		**99.1**	93.5	**100**	**100**	87.5
IV (A,B,C,D), E	*Sen*	91.5	77.4	85.1	**100**	66.1
	Spec	**98.1**	**98.1**	**99.2**	**100**	**99.8**
Accuracy		96.8	94	96.4	**100**	93.1
V D, E	*Sen*	93.8	97.7	97.3	**100**	**100**
	Spec	92.3	85.8	83.9	**100**	**100**
Accuracy		93.1	91.7	90.6	**100**	**100**

The EEG segments falsely classified as *inter-ictal* and *seizure* can be easily discarded by a neurologist. In addition, the overall accuracy achieved for IMF 3 is also acceptable, about 80%. For Case II, 100% sensitivity is achieved for IMF3 with an overall accuracy of 100%, thus indicating a perfect classification of *healthy*, *inter-ictal* and *seizure* groups. In Case III, similar results are obtained for both IMF 2 and IMF 3. Note that this case is closely related to epilepsy diagnosis based on the presence of seizure activity only. In Case IV, 100 % sensitivity and specificity are obtained with IMF 3, indicating exact 9dentification of true positive and negative events. The overall accuracy is also

100%. As for the last case, which is especially important during on-line detection of seizure occurrence for an epileptic patient, 100% sensitivity, specificity and accuracy are achieved using IMF 3 and IMF 4. Table 2.7 provides a comparative study of the obtained results for the various cases with those of several state-of-the-art methods reported in the literature. For the different methods in Table 2.7, the values of the corresponding maximum accuracy are used for comparison.

It is seen that the proposed method shows a better accuracy in most of the cases as compared to those of others. In Case I the accuracy is 80% as compared to the 97.72% accuracy of [18]. This is mainly due to the misclassification of healthy groups (A and B) into the epileptic ones (C, D and E). Thus, it would not strongly affect the detection process. In addition, the proposed method uses feature vectors of lower dimensionality as compared to [18], thus incurs a reduced computational effort.

For example, to extract features from a 4097-point length EEG segment, the time taken by the proposed method is about 0.3 second, whereas the method in [18] requires minimum 3 second and maximum 28 second. Note that an EEG segment is divided into sixteen 256-length blocks and the feature vectors are obtained from the IMFs of different blocks. Since a feature vector is generated from an IMF of a block, the corresponding extraction time is about 0.3/16 second or 19 ms.

Table 2.7: Comparison of classification performance obtained for various algorithms

Case	Method	Feature and classifier	Number of features used	Accuracy (%)
I (A,B), (C,D), E	Tzallas *et al.*[18] (2007)	Fractional energy from TFA, ANN	40	97.72
	Proposed	**EMD, higher order moments, ANN**	**3**	**80**
II A, D, E	Tzallas *et al.*[18] (2007)	TFA, ANN	13	99.28
	Liang *et al.*[14] (2010)	TFA, ApEn, PCA, RBFSVM	16	98.67
	Proposed	**EMD, higher order moments, ANN**	**3**	**100**
III A, E	Tzallas *et al*. [19] (2009)	RI, ANN	16	100
	Bedeeuzzaman *et al*. [16] (2010)	Higher order statistics, Linear classifier	4	97.75
	Fathima *et al.*[17] (2011)	Higher order statistics, Linear classifier	3	96.9
	Proposed	**EMD, higher order moments, ANN**	**3**	**100**
IV (A,B,C, D), E	Tzallas *et al.*[18] (2007)	SPWV dist., ANN	16	97.73
	Liang *et al.*[14] (2010)	TFA, ApEn, PCA, RBFSVM	16	98.51
	Proposed	**EMD, higher order moments, ANN**	**3**	**100**
V D, E	Liang *et al.*[14] (2010)	TFA, ApEn, PCA, RBFSVM	16	98.74
	Proposed	**EMD, higher order moments, ANN**	**3**	**100**

2.6 Summary

In this chapter, a seizure detection method based on using the higher order statistical moments such as variance, skewness and kurtosis has been discussed. An extensive analysis has been carried out in the EMD domain to investigate the ability of these moments in distinguishing the EEG signals. These moments have been used as features to classify the EEG signals using an ANN. A publicly available comprehensive database has been used to study the performance of the proposed method for various classification categories and compare it with that of several recent techniques. It has been shown that the proposed method can provide very high degree of sensitivity, specificity as well as accuracy especially in the case of discriminating seizure activities from the non-seizure ones with reduced computational effort.

CHAPTER 3

EEG SIGNAL DISCRIMINATION USING NON-LINEAR DYNAMICS IN THE EMD DOMAIN

3.1 Overview

In this chapter, a nonlinear approach, based on chaos analysis of EEG signals in the EMD domain, to classify healthy persons, and epileptic patients with and without seizure attacks, is introduced [29]. The signals are discriminated using the values of the largest Lyapunov exponent (LLE) and correlation dimension (CD) calculated from the corresponding IMFs. Using the five sets of EEG signals [25, 26] mentioned in Sec. 2.3, a comprehensive analysis is carried out in the EMD domain and the results show that the values of LLE and CD can be an effective tool for discriminating EEG signals.

As mentioned in Sec. 1.5, these chaotic features, when obtained from the wavelet subbands of the EEG signals are shown to be effective in differentiating the signals of various classes including those of seizures [11]. However, the discriminations are not consistent for different sub-bands and satisfactory performance is achieved for only one sub-band. Concurrently, Lyapunov spectra have been used in [13] to make a multi-way classification using multi-class support vector machines (SVM). In [15], applicability of another chaotic measure named fractal dimension (FD) with SVM is analyzed to classify healthy, inter-ictal and ictal EEG segments.

3.2 EEG Signal Analysis with Chaos

The first step in the chaos analysis is to obtain a phase space portrait, by using the time-dependent variables of the system (here, the EEG signal and its IMFs) as the components of the vectors, constituting the multidimensional phase space of the system. The sequential plots of the time-dependent vectors represent the evolution of the system's state over time. For an N-point data, $\{x_1, x_2, ..., x_N\}$, the phase space portrait having M embedding vectors are reconstructed employing the method of delay coordinates [30]. First, a matrix $\boldsymbol{X}$ is formed as

$$X = \begin{bmatrix} X_1 \\ X_2 \\ \vdots \\ X_n \\ \vdots \\ X_M \end{bmatrix}_{(M\times 1)} = \begin{bmatrix} x_1 & x_{1+l} & \cdots & x_{1+(D-1)l} \\ x_2 & x_{2+l} & \cdots & x_{2+(D-1)l} \\ \vdots & \vdots & \cdots & \vdots \\ x_n & x_{n+l} & \cdots & x_{n+(D-1)l} \\ \vdots & \vdots & \cdots & \vdots \\ x_M & x_{M+l} & \cdots & x_N \end{bmatrix}_{(M\times D)} \tag{3.1}$$

where, $\boldsymbol{X_n}$ represents the *n*-th embedding vector and, $M = N - (D\text{-}1)l$. *D* represents the *embedding dimension* and *l* represents the *lag* or *reconstruction delay*. In order to observe the attractor dynamics from the phase space portrait, the optimum value of lag, and the minimum value of embedding dimension are determined using the algorithm of equidistant histogram box and Cao's method, respectively [31]. Fig. 3.1 and 3.2 show the 3-dimensional phase space portrait of EEG signals recorded from a healthy person and an epileptic patient during inter-ictal and ictal period.

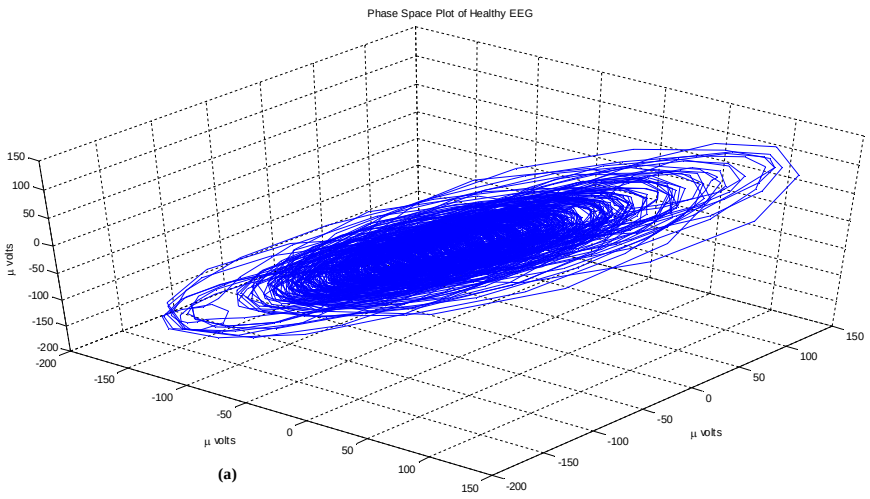

Fig. 3.1: Phase space plot of (a) healthy EEG.

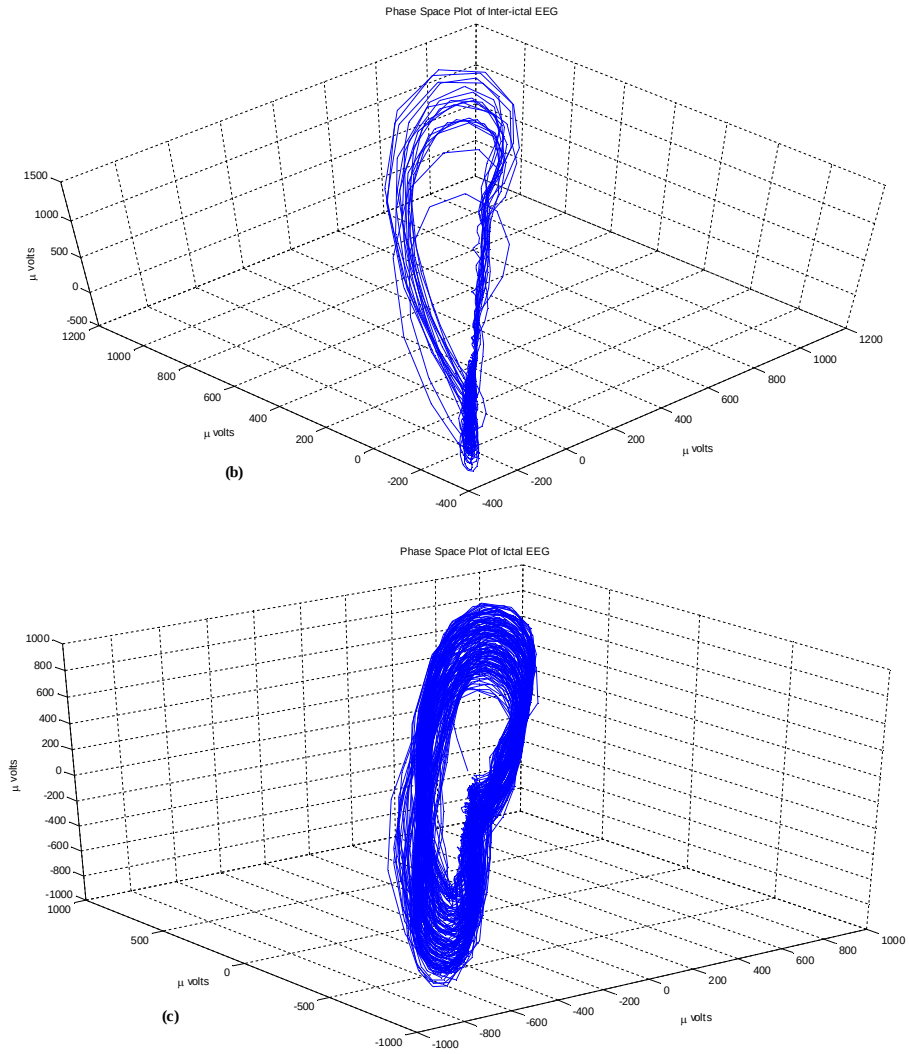

Fig. 3.2: Phase space plot of (b) inter-ictal and (c) ictal EEG.

From Fig. 3.1 and 3.2 it we can see three distinctive phase space portrait for three types of EEG. Furthermore the portrait is more defined for ictal EEG than both the healthy and inter-ictal one. Hence, chaotic measures based on the reconstructed phase space may reveal important nonlinear properties which may help to further improve epilepsy diagnosis and seizure detection system.

It should be noted that the phase space portrait corresponds to the dynamics of an attractor, confined to a sub-region of the system. The attractor is characterized by its level of chaoticity and complexity. The Lyapunov exponents are used as a measure of the chaoticity of the attractors. The exponents quantify the average exponential separation between the nearby trajectories of a phase space. An exponential divergence

coupled with folding of the trajectories represents deterministic randomness and unpredictability. Thus, a positive Lyapunov exponent for almost all initial conditions in a bounded dynamical system is used as an indicator of deterministic chaos.Various methods are proposed to date for obtaining the Lyapunov exponents from a time series data. In the direct method proposed by Wolf et al. [32], the largest Lyapunov exponent (LLE) of a time-series data is obtained as

$$LLE = \frac{1}{n_N - n_0} \sum_{k=1}^{N} \log_2 \left(\frac{L'_k}{L_{k-1}} \right) \tag{3.2}$$

Where

n_0 = initial discrete time instant; n_N, = final discrete time instant,

L_{k-1} = distance between two nearest neighbours on separate trajectories at n_{k-1},

L'_k = distance at time n_k between those two neighbours as evolved from L_{k-1}

and N represents the number of replacement steps. However, the LLE can also be estimated from $p(i)$ vs. i plot [33], where $p(i)$, the prediction error is given by

$$p(i) = \frac{1}{NT_s} \sum_{k=1}^{N} \log_2 \left(\frac{L_{k+i}}{L_k} \right) \tag{3.3}$$

where, i and T_s represents the number of time steps and sampling interval, respectively. According to this method the plot is observed to identify the portion through which the prediction error increases at almost constant rate. Least-square method is used to fit a straight line to this portion and the LLE is estimated as the slope of this straight line, in this thesis, the method of [33] is used since it involves less computational complexity as compared to that of [32].

There is another measure called the correlation dimension (CD) which defines the level of complexity of the attractor. To obtain CD, the correlation sum $C(r)$ is first calculated using the Grassberger-Procaccia algorithm as [34]

$$C(r) = \frac{2}{(N-D+1)(N-D+1-w)} \sum_{j=D}^{N} \sum_{k<j-w} \Theta\left(r - \left|X_j - X_k\right|\right) \tag{3.4}$$

where, r= cell size, w = Theiler window

and Θ = Heaviside step function, $\Theta(x) = \begin{cases} 0; x < 0 \\ 1; x \geq 0 \end{cases}$

Next, the optimum value of CD is obtained employing the Takens-Theiler estimator as [35]

$$CD = \frac{C(r)}{\int_0^r \frac{C(r')}{r'} dr'} \tag{3.5}$$

3.3 Results and Discussion

As discussed in Sec. 2.3, after low-pass filtering, each EEG signal of the available five sets is empirically decomposed into nine IMFs. Using eqn. (3.3), the values of LLE are calculated for the band-limited EEG signals as well as for the corresponding IMFs. For each dataset, the mean and standard deviation (SD) of the values of LLE are then obtained and listed in Table 3.1 for different datasets. The values of CD are obtained using (3.4) and (3.5) and the corresponding mean and SD values are provided in Table 3.2

Table 3.1: Mean values of LLE (SD shown in parenthesis)

Signals	Set A	Set B	Set C	Set D	Set E
Band-Limited	18.16 (2.098)	22.16 (1.93)	11.72 (2.643)	12.89 (3.762)	20.49 (3.634)
IMF 1	24.63 (0.763)	24.09 (0.792)	23.99 (0.898)	23.39 (1.028)	22.14 (2.244)
IMF 2	26.4 (1.253)	26.06 (1.315)	26.68 (1.407)	26.15 (1.914)	25.58 (2.47)
IMF 3	27.69 (1.337)	26.8 (1.422)	26.46 (1.406)	25.88 (2.057)	25.58 (2.863)
IMF 4	21.52 (2.065)	20.75 (2.137)	19.35 (1.903)	19.19 (2.29)	19.49 (3.461)
IMF 5	12.68 (1.901)	11.97 (2.41)	11.39 (2.204)	11.96 (2.487)	11.91 (3.448)
IMF 6	5.665 (2.253)	4.711 (1.999)	4.295 (1.957)	4.757 (2.051)	4.957 (2.551)
IMF 7	1.479 (1.152)	1.681 (1.569)	1.327 (1.176)	1.358 (1.444)	1.396 (1.399)
IMF 8	0.697 (0.667)	0.833 (0.894)	0.583 (0.809)	0.644 (0.74)	0.551 (0.858)
IMF 9	0.142 (0.385)	0.179 (0.495)	0.029 (0.118)	0.093 (0.248)	0.141 (0.32)

It is observed from Table 3.1 that the mean value of LLE shows no specific trend for the EEG signals from Set A to Set E and thus, no decision can be taken from it. However, it decreases as one move from Set A to Set E for IMFs 1 and 3. A similar trend is found

for the IMFs 2 and 4, with an exception for Sets C and D, and Set E, respectively. On the other hand, no specific trend is seen for the IMFs 5 to 9. But, for all IMFs it is seen that the mean value of LLE for Set A is always greater than that for Set E (seizure activity). From Table 3.2 it is observed that the mean value of CD decreases from Set A to Set E for the IMFs 1, 2, 3, 4 and 7, but no general trend for the EEG signals. As for other IMFs, no decision can be taken based on the mean value of CD since it does not show any specific trend.

Table 3.2: Mean values of CD (SD shown in parenthesis)

Signals	Set A	Set B	Set C	Set D	Set E
Band-Limited	13.8 (26.6)	20.47 (101.9)	6.906 (1.572)	6.289 (1.475)	5.252 (1.793)
IMF 1	6.627 (1.356)	6.165 (0.833)	5.769 (0.798)	4.891 (1.264)	4.346 (1.219)
IMF 2	4.682 (0.407)	4.189 (0.478)	4.049 (0.395)	3.858 (0.611)	3.739 (0.829)
IMF 3	3.073 (0.221)	2.907 (0.317)	2.729 (0.231)	2.71 (0.319)	2.702 (0.488)
IMF 4	2.16 (0.122)	2.111 (0.14)	2.079 (0.112)	2.075 (0.126)	2.074 (0.244)
IMF 5	1.874 (0.146)	1.807 (0.206)	1.845 (0.142)	1.815 (0.196)	1.771 (0.239)
IMF 6	1.551 (0.221)	1.483 (0.241)	1.505 (0.222)	1.495 (0.248)	1.451 (0.262)
IMF 7	1.268 (0.182)	1.264 (0.166)	1.252 (0.148)	1.25 (0.159)	1.23 (0.165)
IMF 8	1.182 (0.085)	1.171 (0.088)	1.174 (0.085)	1.168 (0.094)	1.143 (0.148)
IMF 9	1.095 (0.136)	1.098 (0.07)	1.003 (0.282)	1.084 (0.13)	1.072 (0.204)

Furthermore, a one-way analysis of variance (ANOVA) is performed at 99% confidence level, where no significant difference among the means of the five data sets represents a null hypothesis. The null hypothesis will be rejected if the corresponding p value is less than 0.001. Table 3.3 shows the results obtained from the ANOVA.

Table 3.3: *p*-values obtained from one way ANOVA

Signals	*p*-value for LLE	*p*-value for CD
Band-Limited	**0**	0.1095
IMF 1	**0**	**0**
IMF 2	**0.0002**	**0**
IMF 3	**2.3908e-14**	**0**
IMF 4	**1.59983e-13**	**0.0002**
IMF 5	0.0113	0.0021
IMF 6	0.0003	0.0579
IMF 7	0.3593	0.5238
IMF 8	0.104	0.0812
IMF 9	0.02	0.0017

It is seen from Table 3.3 that the null hypothesis is rejected for both the LLE and CD in the case of the IMFs 1, 2, 3 and 4. Thus, the LLE and CD values of the five sets are significantly different from each other if their first four IMFs are considered. This is further illustrated in Fig. 3.2, 3.3 and 3.4 that show the confidence interval plots for the EEG signals and the corresponding first two IMFs. Fig. 3.2 shows plots for original band-limited EEG signals whereas Figs. 3.3 and 3.4 the plots for first and second IMFs, respectively. Notice that, the LLE values calculated directly from the signal shows discriminating feature but in an inconsistent manner, while the values of CD are all similar, thus useless for discrimination. On the other hand, the values of CD and LLE obtained from the IMFs clearly show distinguishing feature-enabling one to easily discriminate signals belonging to various categories including seizure-free intervals and seizure attacks. Overall, it is clear that the values of LLE and CD can be quite effectively employed to identify seizure activities from the various IMFs of the EEG signals. In addition, one can take decisions from multiple IMFs, which is more convincing.

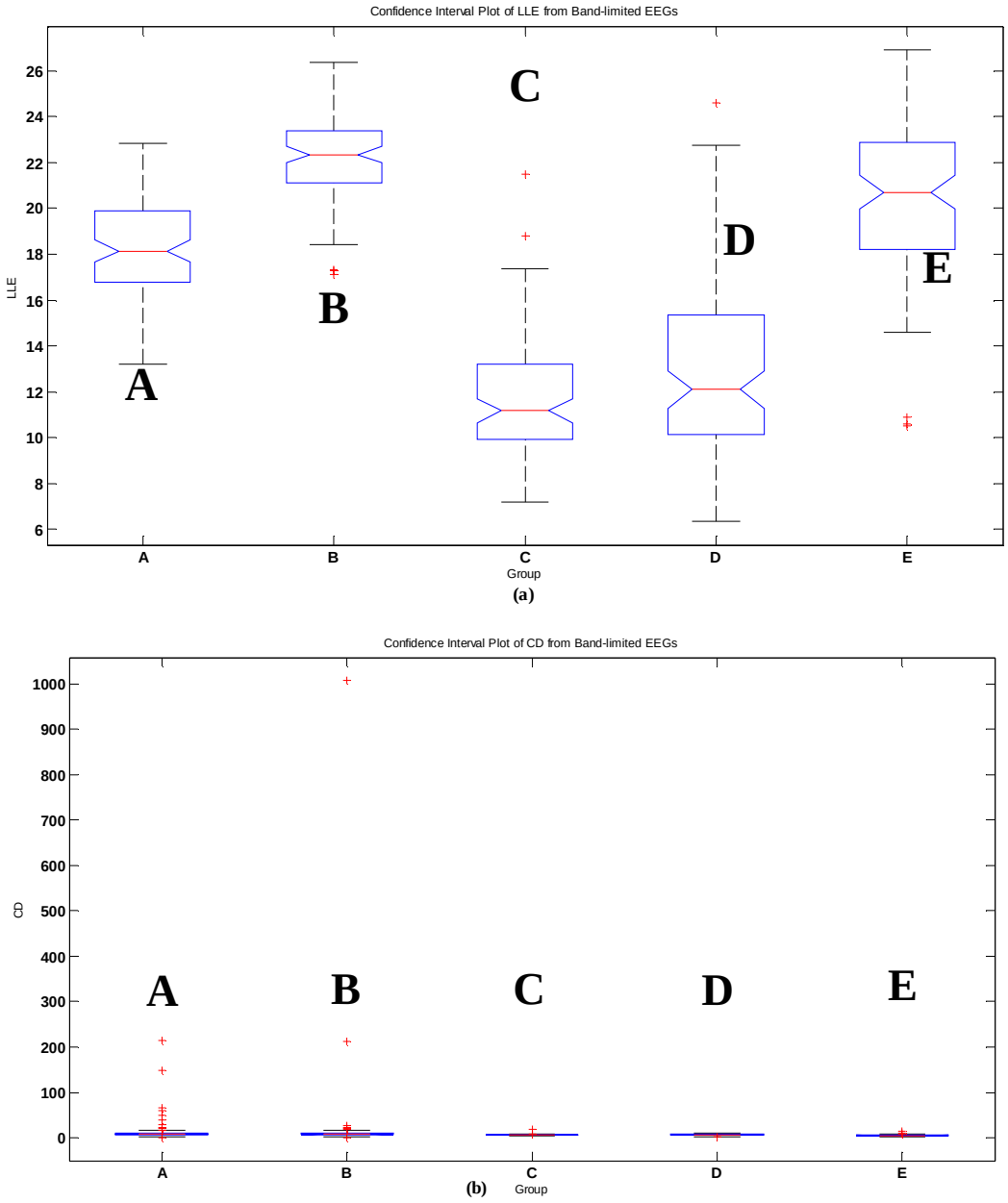

Fig. 3.3: Confidence interval plots of (a) LLE and (b) CD from band-limited EEGs

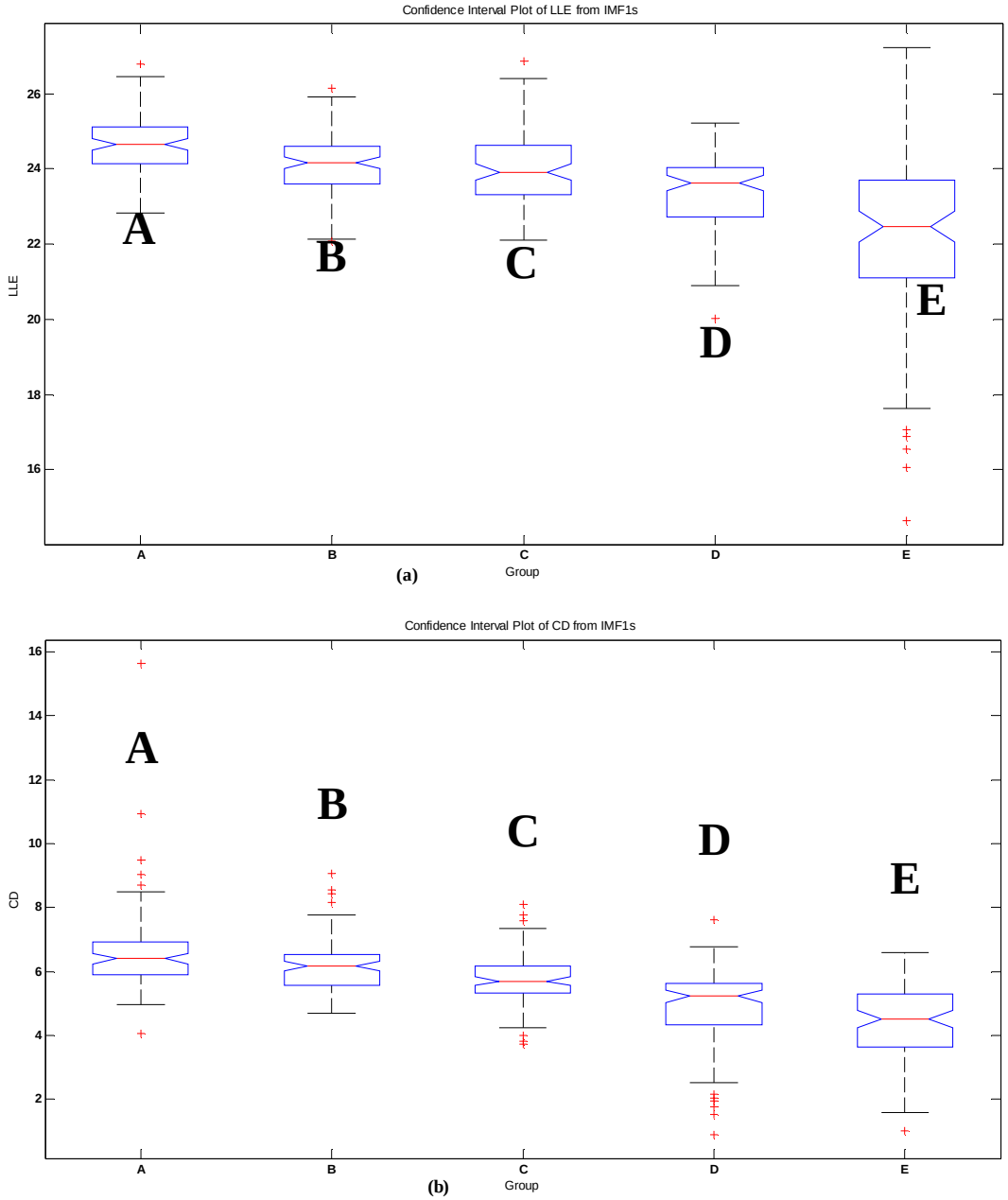

Fig. 3.4: Confidence interval plots of (a) LLE and (b) CD from IMF1s

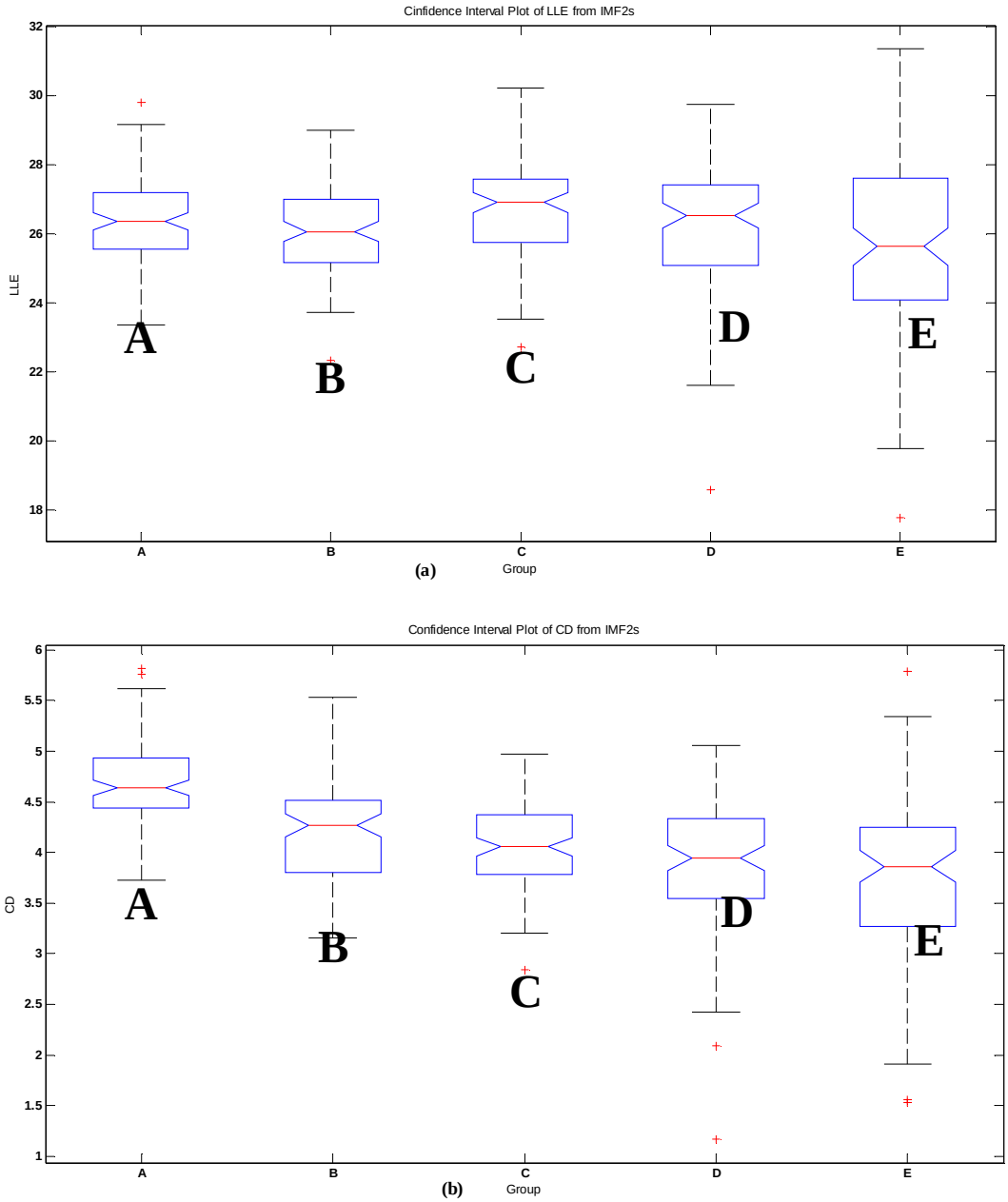

Fig. 3.5: Confidence interval plots of (a) LLE and (b) CD from IMF2s

3.4 Summary

EEG signals have been analysed using chaotic parameters in the EMD domain to differentiate the signals of healthy and epileptic patients. The largest Lyapunov exponent (LLE) and correlation dimension (CD) have been employed as the measure of chaoticity and complexity of a signal, respectively, and calculated for various IMFs of a large group of EEG signals of healthy and epileptic persons (with and without seizure attacks). It has been observed that both the value of LLE and CD decreases as the non-linearity as well as randomness of IMF decreases from healthy to signals corresponding to seizure activity. Thus, the parameters have demonstrated distinguishing features enabling one to discriminate the EEGs of seizure attacks from the others.

CHAPTER 4

DETECTION OF EPILEPTIC SEIZURES USING CHAOTIC AND STATISTICAL FEATURES IN THE EMD DOMAIN

4.1 Overview

As discussed in Chapter 1, 2 and 3, EMD is quite suitable for nonlinear signals like EEG. Also, the statistical and chaotic features exhibit discriminating characteristics for first four IMFs. For this reason, three statistical features, variance, skewness and kurtosis will be calculated using eqn. (2.10), (2.11) and (2.12), respectively. Two chaotic features, LLE and CD will be calculated using eqn. (3.3) and (3.4), (3.5), respectively. In addition to that, another chaotic measure called approximate entropy (ApEn) will be calculated from the band-limited EEGs as well as first four IMFs.

The objective of this chapter is to develop classification method using a combination of both statistical and chaotic features as patterns for classification by a neural network [36]. It is worthwhile to mention that to the best of our knowledge, the application of the statistical features and ApEn in EEG signal discrimination in the EMD domain is still not reported in the literature.

Entropy is a thermodynamic quantity that describes the amount of disorder in the system. It is estimated from a time series using either power spectral analysis or phase space reconstruction. It is shown in [14] that the ApEn can effectively characterize the complexity of EEG signals and thus, may be used as a feature suitable for their classification. For an EEG data, the approximate entropy (ApEn) is given by [37]

$$ApEn(D,r,N) = \frac{1}{N-D}\sum_{i=1}^{N-D}\log C_i^{D+1}(r) - \frac{1}{N-D+1}\sum_{i=1}^{N-D+1}\log C_i^{D}(r) \qquad (4.1)$$

where $C_i^D(r)$ represents the correlation integral with D embedding dimension and time lag of 1 sample. Larger values of ApEn indicate higher irregularity in a time series. In this analysis, D is set to 2 and r is set to the 15% of standard deviation of each time series [38].

Table 4.1 gives the mean and SD values of ApEn obtained for band-limited EEG signals and their corresponding IMFs. It is observed that for a particular group, the mean values

of ApEn decreases as one move from band-limited EEGs to their corresponding IMFs. It can also be observed that, for a particular IMF as well as the band-limited EEGs, the highest mean is obtained for Set A and the lowest for Set E, indicating the reduction of randomness of EEGs when seizure occurs. Furthermore, a gradual reduction of the mean values from Set A to Set E can be noticed for band-limited EEGs, and first two IMfs.

Table 4.1: Mean values of ApEn (SD shown in parethesis)

Signals	Set A	Set B	Set C	Set D	Set E
Band-limited	0.6899 (0.058)	0.621 (0.065)	0.566 (0.065)	0.532 (0.103)	0.479 (0.091)
IMF1	0.548 (0.049)	0.526 (0.047)	0.542 (0.051)	0.508 (0.077)	0.505 (0.077)
IMF2	0.5071 (0.034)	0.499 (0.039)	0.502 (0.038)	0.491 (0.055)	0.478 (0.072)
IMF3	0.4547 (0.059)	0.436 (0.066)	0.411 (0.069)	0.406 (0.072)	0.414 (0.08)
IMF4	0.2604 (0.08)	0.246 (0.083)	0.211 (0.074)	0.22 (0.081)	0.235 (0.094)
IMF5	0.0882 (0.049)	0.082 (0.049)	0.071 (0.04)	0.077 (0.046)	0.087 (0.056)
IMF6	0.0322 (0.032)	0.031 (0.031)	0.029 (0.032)	0.03 (0.032)	0.032 (0.032)
IMF7	0.015 (0.026)	0.014 (0.025)	0.012 (0.023)	0.013 (0.025)	0.014 (0.024)
IMF8	0.0071 (0.018)	0.007 (0.017)	0.007 (0.018)	0.007 (0.017)	0.007 (0.018)
IMF9	0.0046 (0.015)	0.005 (0.016)	0.004 (0.014)	0.004 (0.013)	0.005 (0.015)

To investigate the level of discrimination, a one-way ANOVA analysis at 99% confidence interval is carried out for band-limited EEGs and the IMFs. The corresponding *p*-values, given in Table 4.2 and the confidence interval plots (Fig. 4.1) show that, ApEn values are significantly different for band-limited EEGs as well as first five IMFs. Thus, it will be worthwhile to add ApEn as a feature in designing the classification system.

Table 4.2: *p*-values obtained from one-way ANOVA analysis

Signals	*p*-values for ApEn
Band-limited	**0**
IMF1	**0**
IMF2	**0**
IMF3	**0**
IMF4	**0**
IMF5	**0**
IMF6	0.0113
IMF7	0.0341
IMF8	0.7271
IMF9	0.1438

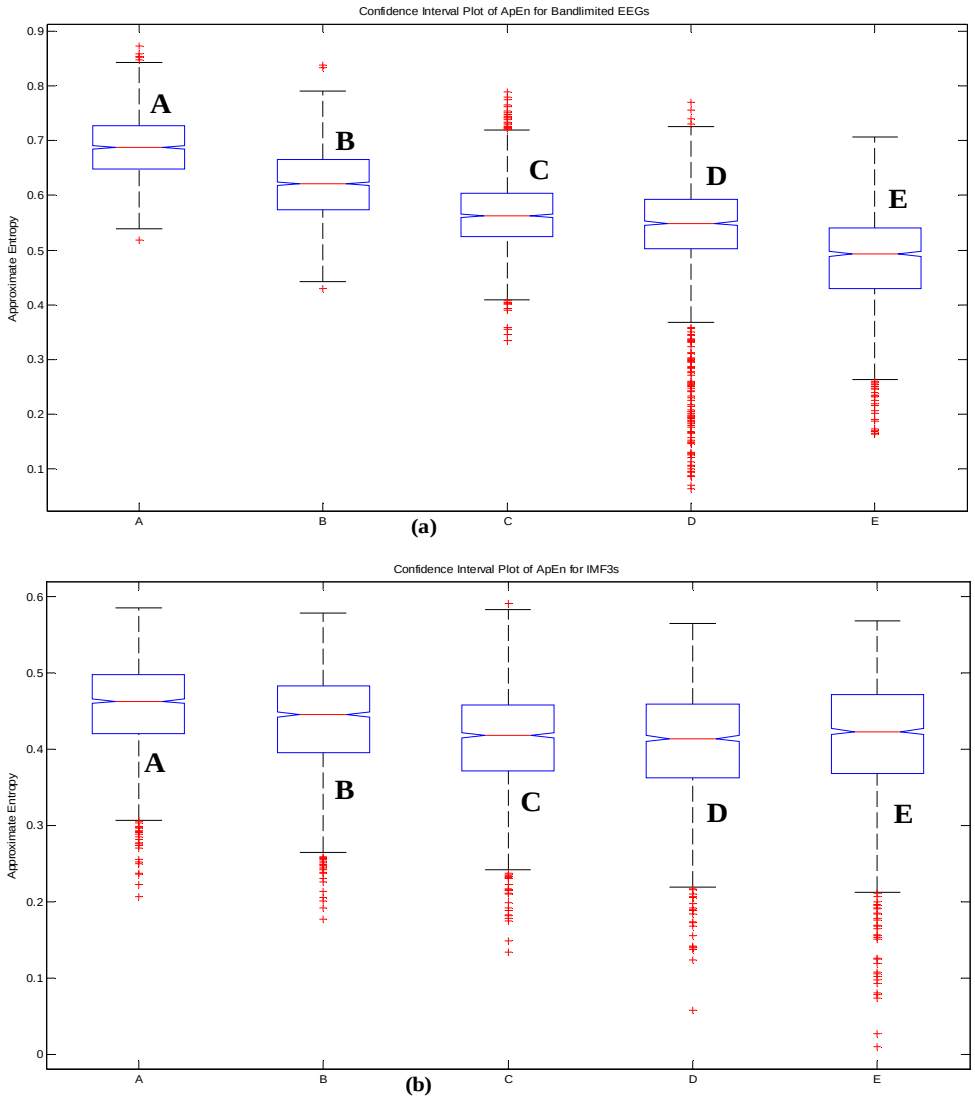

Fig. 4.1: Confidence interval plots for (a) Band-limited EEGs and (b) IMF3s.

4.2 Classification of EEG Signals

The detection of seizure activity from an EEG segment is based on identifying the features that can differentiate it from normal or inter-ictal segments. It is also possible to determine whether a person is suffering from epilepsy or not using the extracted features. In this analysis, EEG segments from Set A, D and E is used which has already been discussed in Sec. 2.3 [25, 26]. After low-pass filtering, each of the EEG segments from three data sets is empirically decomposed into first four IMFs. Due to the non-stationary nature, an IMF is further segmented into 16 blocks using a rectangular window of length 256. For each window three chaotic features (LLE, CD, ApEn) and three statistical features (variance, skewness, kurtosis) are calculated. For the purpose of comparison, features are extracted from band-limited signals, too. Three cases of classification problem are considered. In Case I, Set D and Set E are classified into the *inter-ictal* and *seizure* classes, respectively. In Case II, segments from Set A and Set E are classified into *healthy* and *seizure* classes, respectively. Case I represents the detection of seizure occurrence for an epileptic patient whereas case II represents the diagnosis of whether a person is suffering from epilepsy or not. Case III is a combination of Case I and II. Note that all the three cases are close to real medical scenario.

Since an EEG segment is divided into 16 blocks and there are 100 segments in a set, 1600 feature vectors of dimension six are constructed for a particular set. The classification process is carried out by feeding these feature vectors into a two-layer feed-forward neural network, where the number of neurons is set to 20 in the hidden layer and equal to the number of classes in the output layer. The training, validation and testing for classification are carried out using the well-known MATLAB® software package, where 60%, 5% and 35% of the feature vectors are selected randomly for the purpose of training, validation and testing, respectively. The performance of classification for each case is studied in terms of sensitivity (Sen), specificity (Spec) and accuracy (Acc) using eqn. (2.13), (2.14) and (2.15), respectively.

The values of sensitivity, specificity and accuracy obtained for the proposed method are shown in Table 4.1 for various cases. It is seen that for IMF 3, perfect classification is achieved in almost all the cases.

Table 4.3: Performance of the proposed method

Case		**Band-Limited EEG**	**IMF 1**	**IMF 2**	**IMF 3**	**IMF 4**
I (D, E)	*Sen*	95.375	97.13	97.88	**100**	**100**
	Spec	87.125	86.81	78	**100**	**100**
Accuracy		91.25	91.97	87.94	**100**	**100**
II (A, E)	*Sen*	99.875	89.7	**100**	**100**	95.8
	Spec	99.375	99.4	**100**	**100**	69.9
Accuracy		99.625	94.5	**100**	**100**	82.84
III (A, D, E)	Sen_A	88.125	75.7	84.44	**100**	68
	Sen_D	72.625	61	97.06	**100**	99.06
	Sen_E	74.625	86.2	100	**100**	94.2
Accuracy		78.46	74.3	93.83	**100**	87.1

The performance of classification system can also be visualized using a confusion matrix. It is a matrix having the index of target or actual class as column index and index of the output class as the row index. The content of the *i*th row and *j*th column represents the number of patterns of class *j* classified under class *i*. Fig. 4.2 shows the confusion matrix obtained for case II using the features from IMF 1 and IMF 3. For same IMFs, Fig. 4.3 shows the confusion matrix of case III.

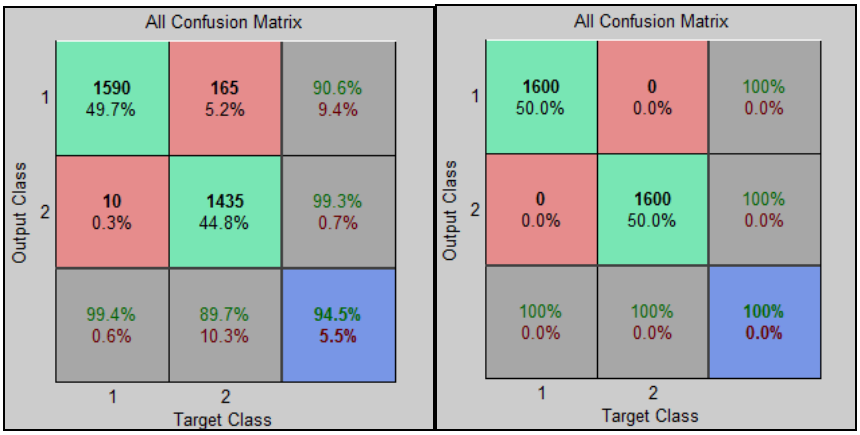

(a) **(b)**

Fig. 4.2: Case II confusion matrix for (a) IMF1s and (b) IMF3s.
(Class 1-*healthy*, Class 2-*ictal*)

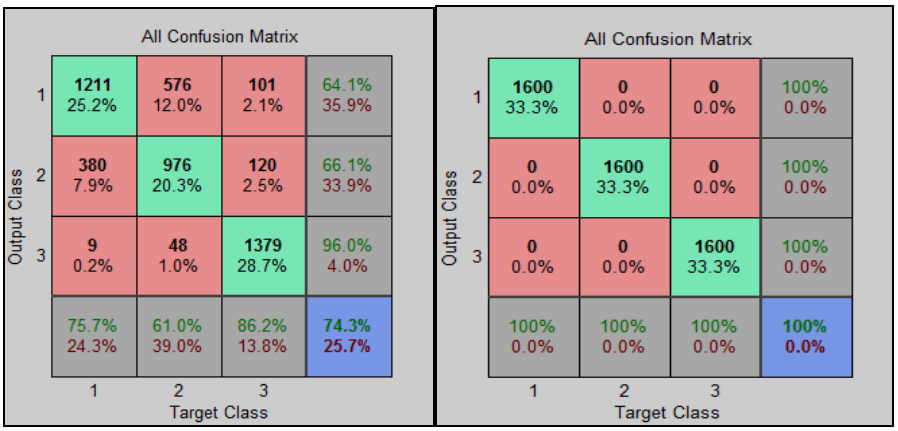

(a) **(b)**

Fig. 4.3: Case III confusion matrix for (a) IMF1s and (b) IMF3s.
(Class 1-*healthy*, Class 2-*inter-ictal*, Class 3-*ictal*)

From Table 4.3, it is seen that for IMF 3, perfect classification is achieved in almost all the cases. The maximum accuracy achieved by the proposed method is compared with that of several recent techniques in Table 4.4. Notice that for the various cases, it gives higher accuracy as compared to the other methods.

Table 4.4: Comparison with other methods

Case	Method	Accuracy (%)
I (D, E)	Liang *et al.*[14]	98.74
	Proposed	**100**
II (A, E)	Tzallas *et al.* [19]	100
	Bedeeuzzaman *et al.* [16]	97.75
	Fathima *et al.*[17]	96.9
	Proposed	**100**
III (A, D, E)	Tzallas *et al.*[18]	99.28
	Liang *et al.*[14]	98.67
	Proposed	**100**

4.3 Summary

A combination of statistical and chaotic features obtained in the EMD domain has been used for classifying EEG signals. Using these features, the classification has been carried out by an ANN. The performance of the proposed method has been investigated for various practical cases using a comprehensive database. It has been shown that the proposed method gives perfect classification in almost all the cases, better than several state-of-the-art techniques.

CHAPTER 5

STATISTICAL MODELING OF EEG SIGNALS IN THE EMD DOMAIN

5.1 Overview

The characteristics of sample distribution of EEG signal can significantly improve the performance of epilepsy diagnosis and seizure detection system. In Chapter 2 we observe this in terms of classification accuracy, which have reached the maximum value (i.e. 100%) in most of the cases. It should be noted that, three features defining the average level of dispersion, asymmetry and peakedness have been used to attain this level of accuracy.

Observing the results in Chapter 2, it would be worth-while to investigate the underlying statistics of EEG data. There are several standard statistical models which are used to fit sample distribution and quantify the overall statistics of data. In this case the estimated model parameters may be used as features in classifying various types of EEG signals, since they will represent the fitted signal as a whole rather being average statistical characteristics. The modeling of a sample distribution is based on the optimum fitting of its probability density using a standard density function where the parameters of the function are estimated from the sample data itself.

In this chapter, two well known standard statistical models named, normal inverse Gaussian (NIG) distribution and stable distribution will be used to fit the distribution of band-limited EEG signals as well as its IMFs. An extensive analysis will be carried out using the same database of EEG signals [25, 26], introduced in Chapter 2. The goodness-of-fit of these modeling will be evaluated in terms of Kullback-Leibler divergence (KLD) and Kolmogorov-Smirnov (KS) statistics.

5.2 The Normal Inverse Gaussian distribution

A random variable X is said to be normal inverse Gaussian (NIG) if its probability density is fitted by the following probability density function (pdf) [39]:

$$f_{NIG}(x;\alpha,\beta,\delta,\mu)=\frac{\alpha}{\pi}\exp\left(\delta\sqrt{\alpha^2-\beta^2}-\beta\mu\right)\frac{K_1\left(\alpha\delta\sqrt{1+\left(\frac{x-\mu}{\delta}\right)^2}\right)}{\sqrt{1+\left(\frac{x-\mu}{\delta}\right)^2}}\exp(\beta x) \qquad (5.1)$$

where, $K_1(.)$ is the first ordered modified Bessel function of the second kind. The density function is valid for the parameters $(\alpha, \beta, \delta, \mu)$ satisfying the following inequality conditions:

$$0 \le |\beta| < \alpha; \delta > 0 \text{ and } -\infty < \mu < \infty \tag{5.2}$$

The parameters are estimated from the data in four steps. In the first step, four lowest order moments about the origin are calculated. For an N-point data, $X\{x_1, x_2, ..., x_N\}$, the rth moment about the origin is defined as

$$m_r = \frac{1}{N}\sum_{i=1}^{N} x_i^r \; ; \; r = 1, 2, 3, 4 \tag{5.3}$$

Next, the first four cumulants are calculated from these moments using the following set of equations

$$\begin{aligned} k_1 &= m_1 \\ k_2 &= m_2 - m_1^2 \\ k_3 &= m_3 - 3m_2m_1 + 2m_1^3 \\ k_4 &= m_4 - 4m_3m_1 - 3m_2^2 + 12m_2m_1^2 - 6m_1^4 \end{aligned} \tag{5.4}$$

Then, four intermediate quantities $(\gamma_3, \gamma_4, \xi, \rho)$ are calculated from these cumulants:

$$\begin{aligned} \gamma_3 &= \frac{k_3}{(k_2)^{3/2}} \\ \gamma_4 &= \frac{k_4}{(k_2)^2} \\ \xi &= \frac{3}{\gamma_4 - \frac{4}{3}\gamma_3^2} \\ \rho &= \frac{\gamma_3}{3}\sqrt{\xi} \end{aligned} \tag{5.5}$$

It should noted that k_1, k_2, γ_3 and γ_4 represent the mean, variance, skewness and kurtosis of the data, respectively.

At the final step, the density parameters $(\alpha, \beta, \delta, \mu)$ are estimated using the following relationships:

$$\delta = \sqrt{k_2 \xi (1-\rho^2)}$$
$$\alpha = \frac{\xi}{\delta\sqrt{1-\rho^2}}$$
$$\beta = \alpha\rho$$
$$\mu = k_1 - \rho\sqrt{k_2\xi} \tag{5.6}$$

For accurate estimation of the parameters using the cumulants, data length *N* should be sufficiently large [39]. Effects of these parameters are illustrated on following figures.

Fig. 5.1 shows the effect of steepness parameter α and scaling parameter δ, keeping both β and μ zero. And Fig. 5.2 shows the effect of skewness parameter β and location parameter μ, keeping both α and δ equal to 1.

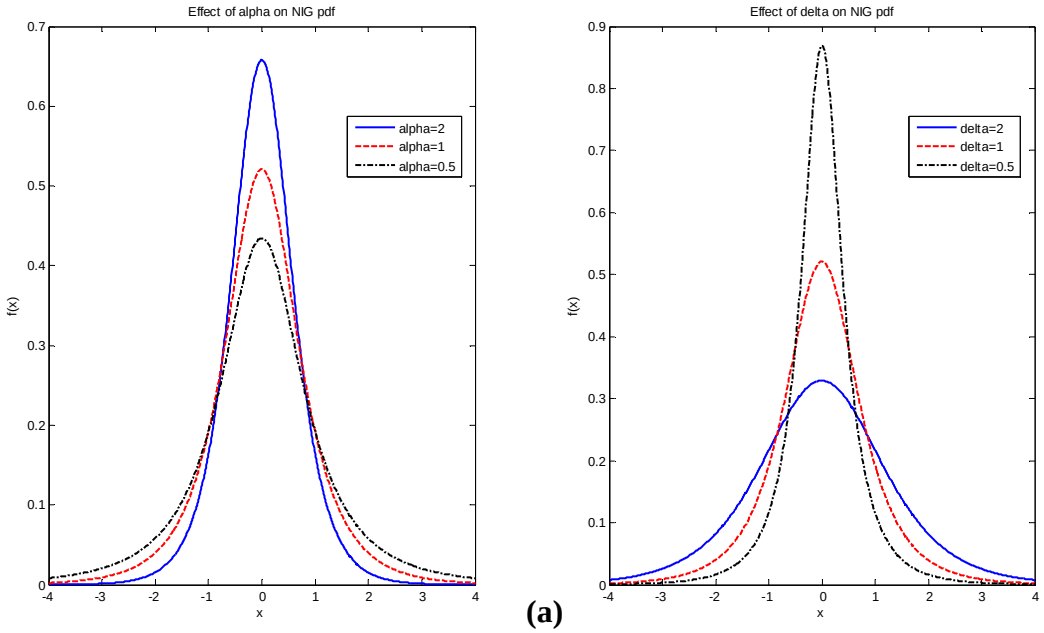

(a)

Fig. 5.1: Effects of α and δ on NIG pdf.

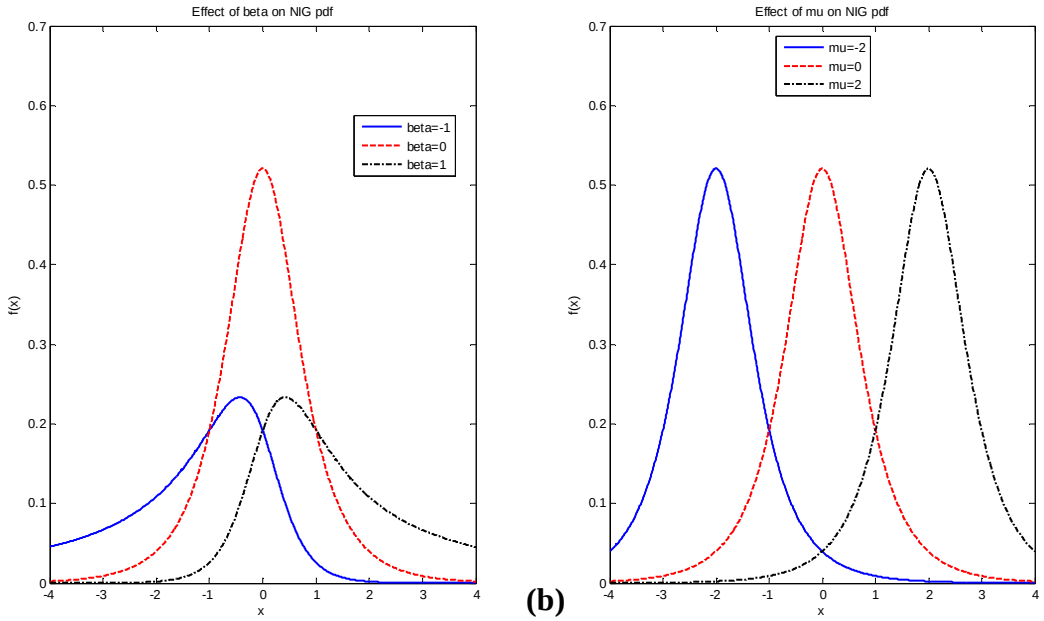

Fig. 5.2: Effects of β and μ on NIG pdf.

5.3 The Stable Distribution

Stable distributions are a rich class of probability distributions, which fit highly skewed and heavy tailed distribution of data. *Normal*, *Cauchy* and *Lévy* are some of the members of this class. A random variable X is said to be *stable* if the shape of its distribution is preserved (upto scale and shift) under addition. The stable pdf of X, $S(\alpha, \beta, \gamma, \delta)$ is defined by the following characteristic function [40]:

$$E\exp(juX) = \begin{cases} \exp\left(-\gamma^{\alpha}|u|^{\alpha}\left[1 - j\beta\left(\tan\frac{\pi\alpha}{2}\right)sign(u)\right] + j\delta u\right); \alpha \neq 1 \\ \exp\left(-\gamma|u|\left[1 + j\beta\frac{2}{\pi}sign(u)\ln|u|\right] + j\delta u\right); \alpha = 1 \end{cases} \quad (5.7)$$

where, α = stability index; $\alpha \in (0,2]$

β = skewness parameter; $\beta \in [-1,1]$

γ = scale parameter; $\gamma \geq 0$

and δ = location parameter; $\delta \in \Re$

In our analysis, the estimation of these parameters as well as calculation of probability density is done using *STBL* toolbox [41].

The effect of these parameters on stable distribution is illustrated on the next page. Fig. 5.3 (a) shows the effect of stability index α and skewness parameter β, keeping γ = 1

and $\delta = 0$. And Fig. 5.3 (b) shows the effect of scale parameter γ and location parameter δ, keeping $\alpha = 1$ and $\beta = 0$.

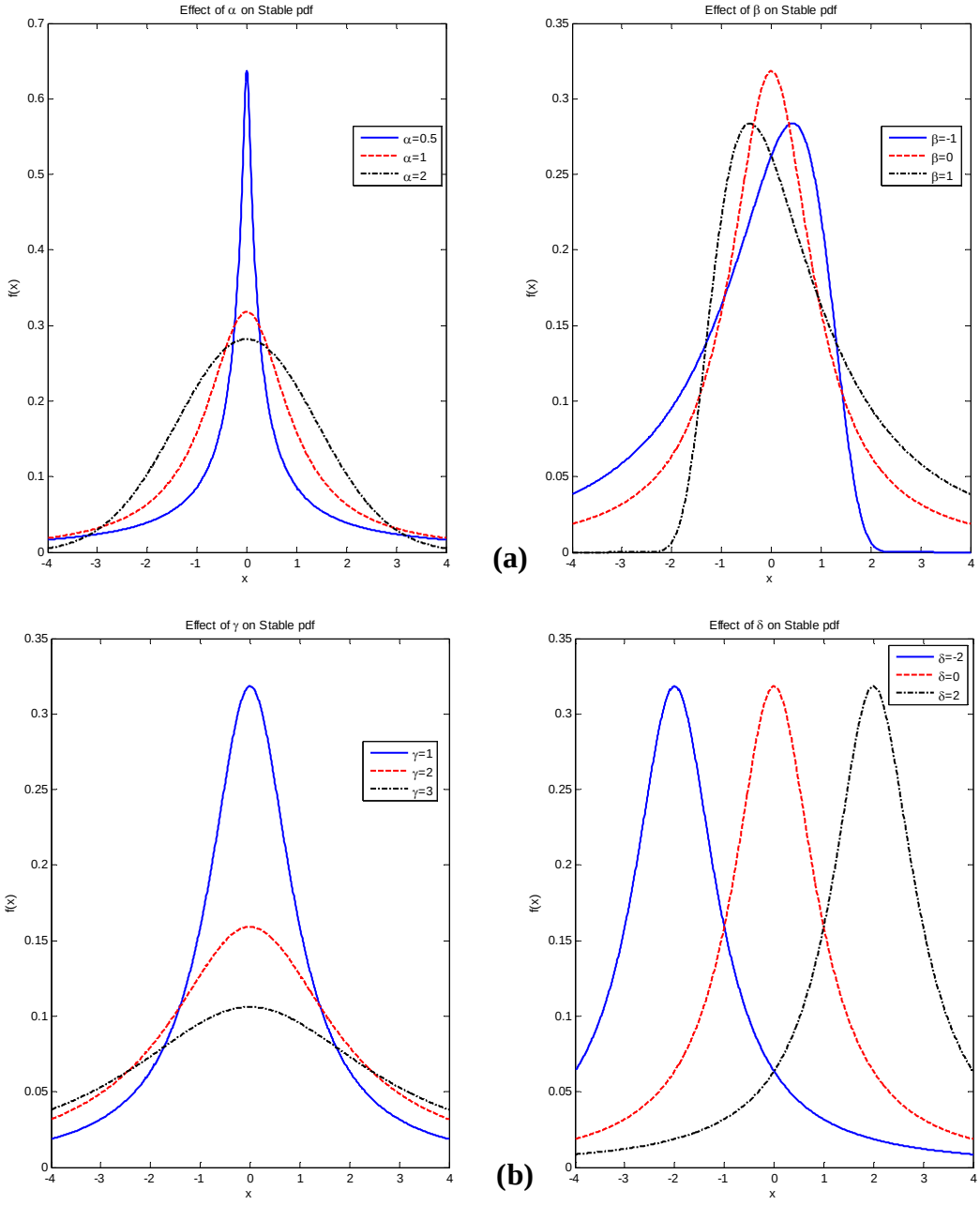

Fig. 5.3: Effects of (a) α, β and (b) γ, δ on Stable pdf.

5.4 Statistical Modeling of EEG signals and its IMFs

As discussed in Sec. 2.3, the EEG signals from each of the five data sets are low-pass filtered using 6^{th} order Butterworth filter and then empirically decomposed into nine IMFs. A histogram plot is obtained for each IMF and band-limited EEG signal so that relative frequency of occurrence can be stored for 512 equally distributed voltage labels.

This information will be used to generate *empirical* pdf, P_{emp}. The procedure is illustrated below for 256 equally distributed voltage labels.

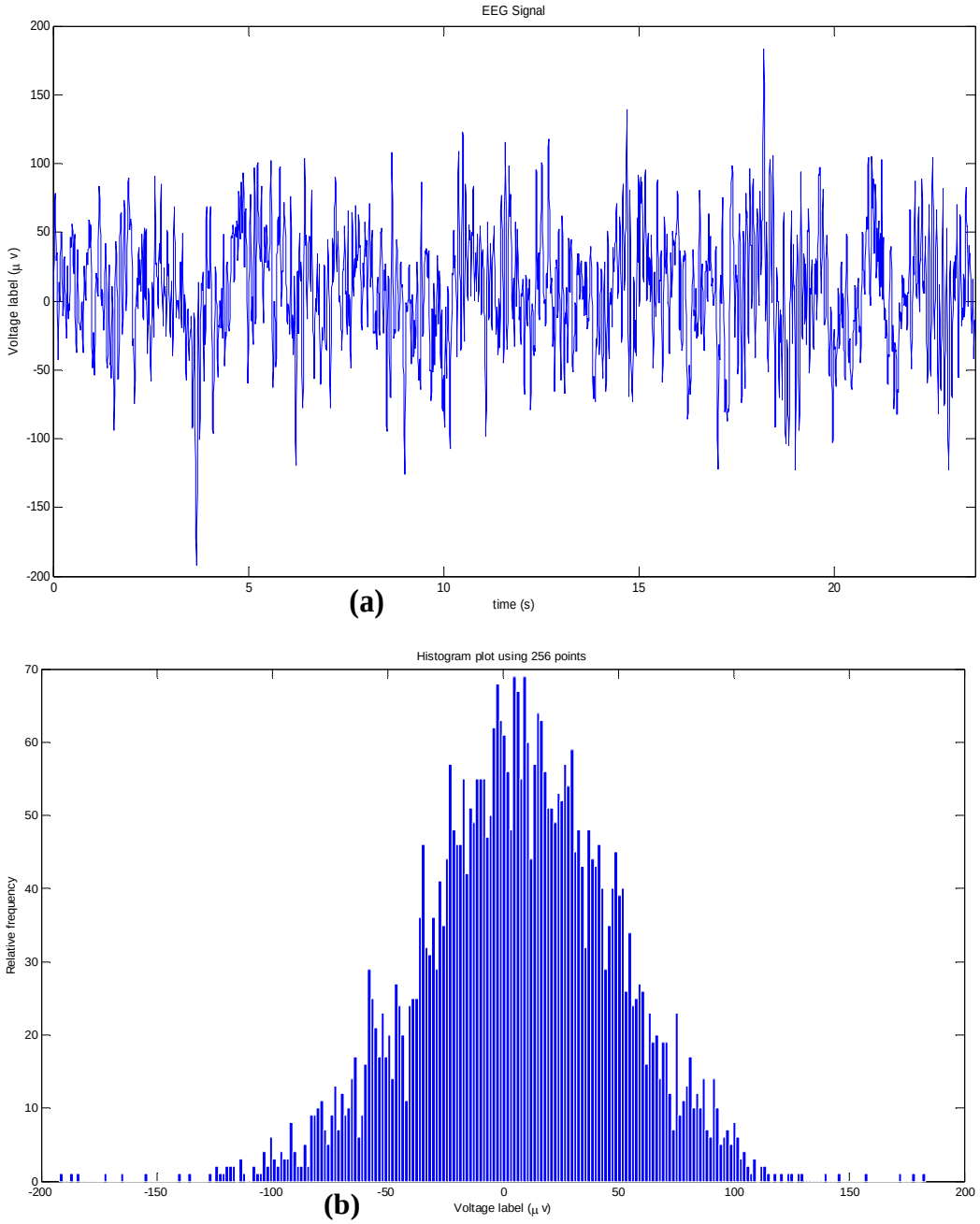

Fig. 5.4: Sample EEG signal (a), and its histogram plot (b).

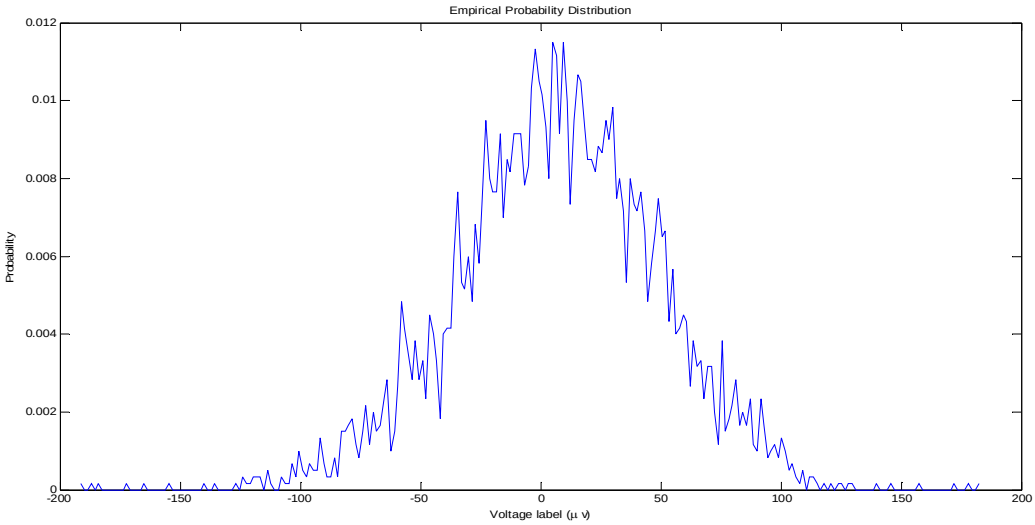

Fig. 5.5: Empirical probability distribution obtained from EEG signal.

The sample EEG signal and its histogram plot are shown in Fig. 5.4. The empirical probability distribution derived from the histogram is shown in Fig. 5.5.The set of equally spaced voltage labels thus obtained, are used to the NIG and stable distributions using eqn. (5.3-5.6) and *STBL* toolbox, respectively.

5.5 Results and Discussions

The fitting of NIG and stable pdf to a sample EEG signal and its corresponding P-P plot is shown below. The P-P plot is a visual tool to observe the goodness-of-fit obtained by a standard pdf. For the empirical pdf, this plot will give a straight line passing through the origin. To what level does the standard P-P plot matches that of empirical pdf, gives an idea of goodness-of-fit. However, visual inspection may not always be correct for P-P plots like Fig. 5.6 (b). For this reason, Kullback-Leibler divergence [42] and Kolmogorov-Smirnov statistics [43] are calculated to numerically quantify the goodness-of-fit.

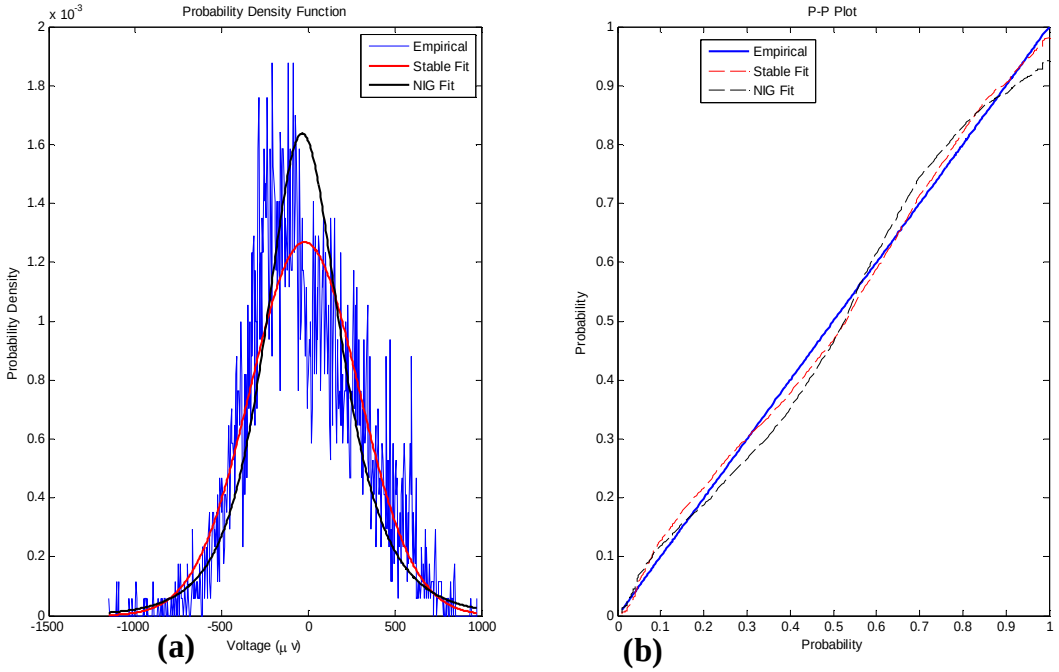

Fig. 5.6: Fitting of NIG and stable pdf (a), and corresponding P-P plot (b).

The Kullback-Leibler divergence (KLD) is given by

$$KLD_{type} = \sum_{x} P_{emp}(x) \log_2 \frac{P_{emp}(x)}{P_{type}(x)} \tag{5.8}$$

where, subscript *type* defines the standard pdf for which the measurement is being carried out. P_{emp} and P_{type} denote the empirical and fitted standard pdfs, respectively. The second quantity, Kolmogorov-Smirnov (KS) statistics is defined as

$$KS_{type} = \max_{x} \left| F_{emp}(x) - F_{type}(x) \right| \tag{5.9}$$

Here, F_{emp} and F_{type} denote the empirical and fitted standard cumulative probability distributions, respectively. For both KLD and KS measures, lower the value, the better is the goodness-of-fit. Fig. 5.7 shows the distribution fitting of a sample EEG signal from Set A. From all the five data sets, each band-limited EEG signal and its nine IMFs are fitted using NIG and stable pdfs. For each case, KLD and KS are measured. Table 5.1 and 5.2 show the mean values of KLDs obtained for fitting NIG and stable pdf, respectively.

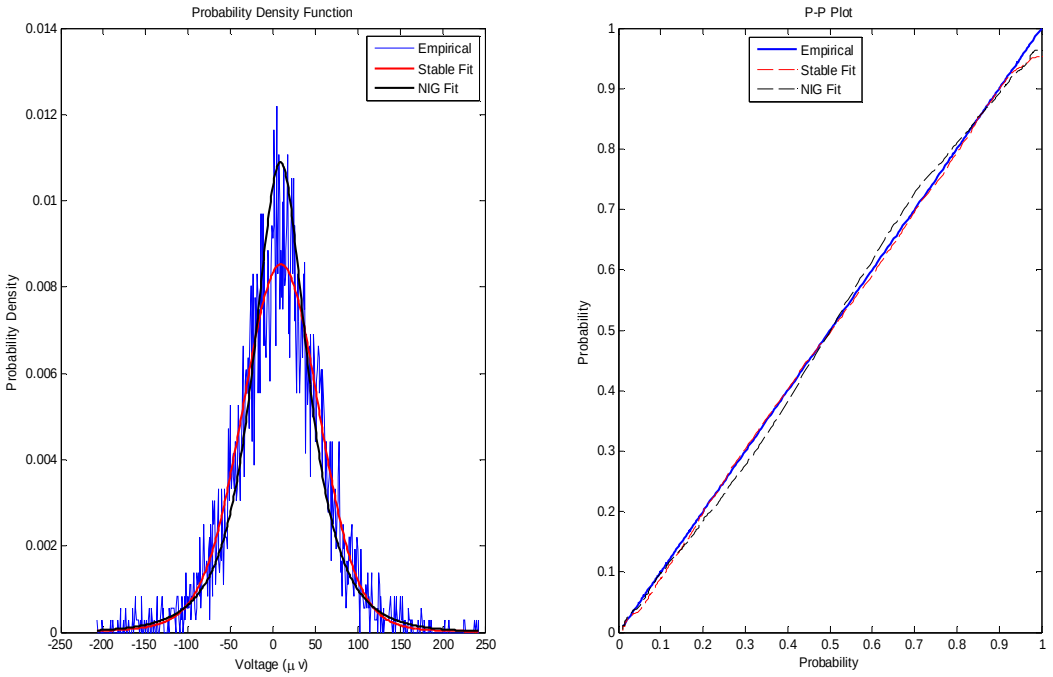

Fig. 5.7: Distribution fitting of a band-limited EEG signal from Set A.

Table 5.1: Mean values of KLD_{NIG} (SD shown in parenthesis)

Signals	Set A	Set B	Set C	Set D	Set E
Band-limited	0.2493 (0.0824)	0.1672 (0.0438)	0.2229 (0.1090)	0.2268 (0.1342)	0.0752 (0.0499)
IMF1	0.3449 (0.1368)	0.1935 (0.0521)	0.4281 (0.2578)	0.4006 (0.2119)	0.0879 (0.0731)
IMF2	0.5320 (0.1749)	0.3627 (0.1228)	0.3851 (0.2150)	0.3743 (0.2050)	0.1079 (0.0856)
IMF3	0.6962 (0.2543)	0.6180 (0.1950)	0.4536 (0.2360)	**0.4847 (0.2795)**	0.1525 (0.0945)
IMF4	0.9473 (0.3426)	0.9290 (0.3372)	0.7567 (0.4254)	0.7699 (0.4517)	0.3201 (0.2509)
IMF5	1.6040 (0.6426)	1.6441 (0.7317)	1.7513 (1.0384)	1.9226 (1.6187)	0.7519 0.6326)
IMF6	4.2048 (2.1928)	3.6301 (1.9723)	4.7522 (3.5697)	4.9823 (3.9804)	1.8763 (1.8647)
IMF7	10.7284 (8.8936)	10.0698 (9.4698)	12.0200 (12.5111)	11.1622 (12.7843)	**3.9639 (4.5583)**
IMF8	21.2369 (22.2463)	16.0529 (16.0468)	15.8035 (14.3168)	17.8704 (24.0495)	6.3093 (7.5020)
IMF9	56.1903 (228.9148)	48.0788 (242.7645)	27.5163 (74.9222)	42.9727 (165.0672)	12.4197 (26.8253)

Table 5.2: Mean values of KLD_{Stable} (SD shown in parenthesis)

Signals	Set A	Set B	Set C	Set D	Set E
Band-limited	0.1721 (0.0519)	0.1176 (0.0319)	0.1697 (0.0730)	0.1644 (0.0875)	0.0690 (0.0428)
IMF1	0.2954 (0.0971)	0.1800 (0.0565)	0.4183 (0.2221)	0.3832 (0.2125)	0.0811 (0.0723)
IMF2	0.4052 (0.1214)	0.2789 (0.0771)	0.3829 (0.1985)	0.3377 (0.1668)	0.0849 (0.0688)
IMF3	0.5624 (0.1746)	0.5039 (0.1370)	0.4198 (0.1949)	**0.6701 (2.3055)**	0.1290 (0.0890)
IMF4	0.8093 (0.2317)	0.7825 (0.2713)	0.6498 (0.3588)	0.6640 (0.3715)	0.2708 (0.2191)
IMF5	1.3911 (0.5228)	1.4748 (0.5671)	1.5281 (0.8837)	1.6613 (1.3142)	0.6674 (0.5327)
IMF6	3.8143 (1.9265)	3.5382 (1.9470)	4.4551 (3.1232)	4.6001 (3.4659)	1.8340 (1.8910)
IMF7	10.3714 (8.3345)	9.2693 (8.2466)	11.3542 (11.6402)	11.1291 (13.0707)	**4.0373 (5.0407)**
IMF8	19.9524 (20.5767)	15.0333 (15.0007)	14.8713 (13.5860)	16.8506 (23.3479)	5.8642 (6.7829)
IMF9	53.6185 (227.4512)	46.0537 (241.3360)	26.1593 (74.1507)	41.6908 (164.1101)	11.7365 (25.8590)

From Table 5.1 and 5.2 it can be observed that, stable pdf fits better than NIG pdf for most the EEG signal types. However, NIG pdf performs better for the 3rd IMFs from Set D and 7th IMFs from Set E. In addition to that, fitting of both standard pdfs is better for band-limited EEGs than for the IMFs for all data sets. Fig. 5.8 and 5.9 below represents the distribution fitting of sample EEG signals from Set D and Set E, repectively.

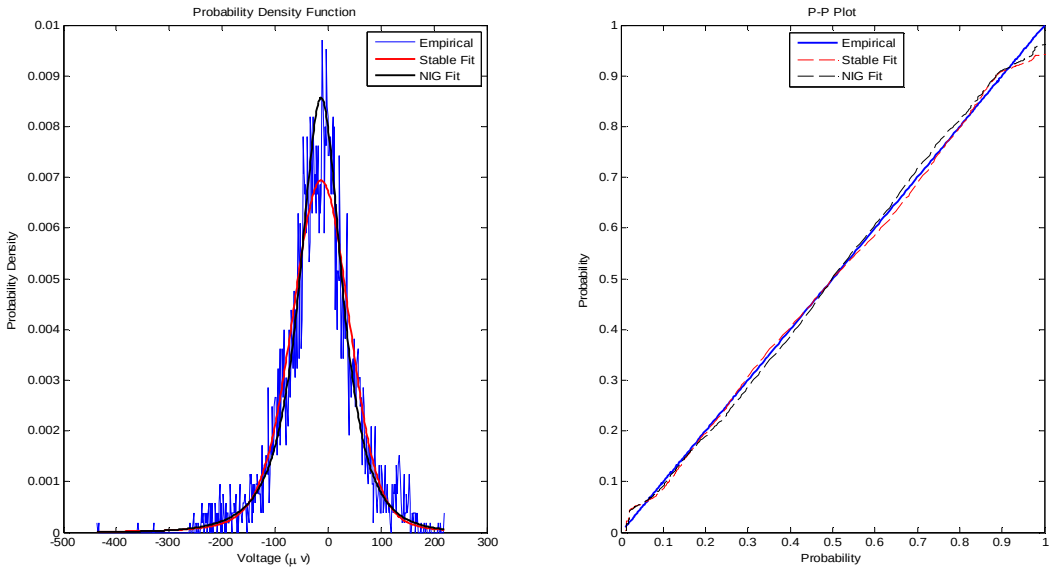

Fig. 5.8: Distribution fitting of a band-limited EEG signal from Set D.

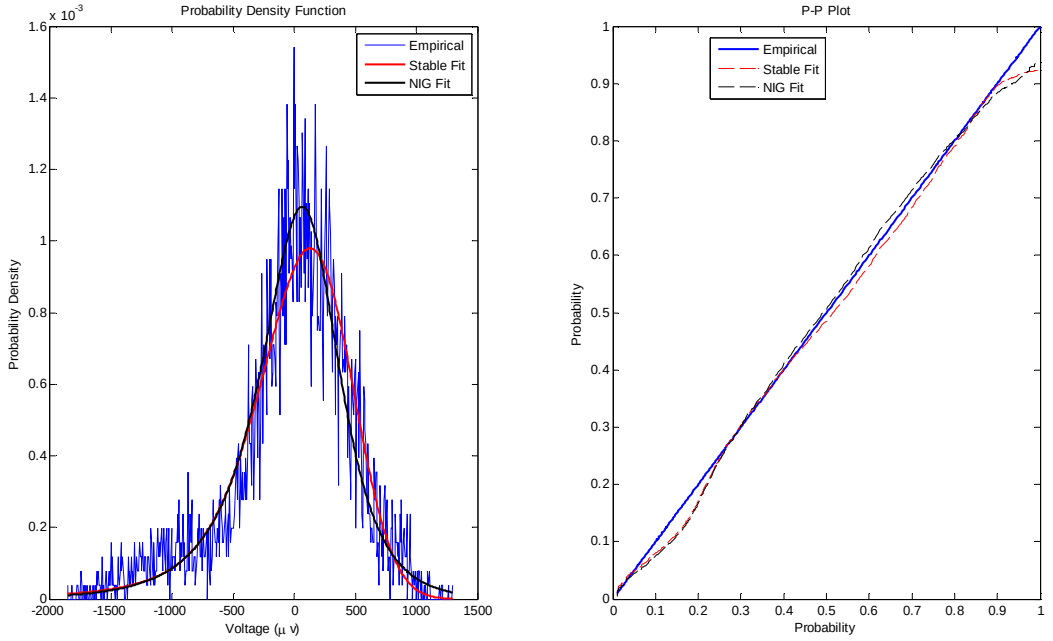

Fig. 5.9: Distribution fitting of a band-limited EEG signal from Set E.

Next we represent the mean values of KS obtained for fitting NIG and stable pdf on Table 5.3 and Table 5.4, respectively.

Table 5.3: Mean values of KS_{NIG} (SD shown in parenthesis)

Signals	Set A	Set B	Set C	Set D	Set E
Band-limited	0.0497 (0.0049)	0.0500 (0.0060)	0.0471 (0.0085)	0.0514 (0.0129)	0.0789 (0.0269)
IMF1	**0.0362 (0.0102)**	**0.0361 (0.0143)**	**0.0294 (0.0142)**	**0.0465 (0.0444)**	**0.0520 (0.0209)**
IMF2	0.0441 (0.0075)	0.0440 (0.0082)	0.0314 (0.0098)	0.0408 (0.0241)	0.0606 (0.0299)
IMF3	0.0452 (0.0097)	0.0444 (0.0093)	0.0378 (0.0110)	0.0433 (0.0182)	0.0512 (0.0224)
IMF4	0.0476 (0.0131)	0.0512 (0.0146)	0.0497 (0.0127)	0.0521 (0.0149)	0.0555 (0.0280)
IMF5	0.0609 (0.0221)	0.0638 (0.0274)	0.0664 (0.0172)	0.0672 (0.0287)	0.0650 (0.0332)
IMF6	0.0930 (0.0376)	0.0960 (0.0358)	0.0953 (0.0338)	0.1024 (0.0412)	0.0972 (0.0549)
IMF7	**0.1358 (0.0478)**	0.1322 (0.0378)	0.1442 (0.0422)	**0.1340 (0.0461)**	**0.1308 (0.0436)**
IMF8	**0.1780 (0.0474)**	**0.1886 (0.0474)**	0.2025 (0.0507)	**0.1905 (0.0462)**	**0.1774 (0.0490)**
IMF9	**0.1924 (0.0426)**	**0.2030 (0.0372)**	**0.1869 (0.0640)**	**0.1805 (0.0679)**	**0.1891 (0.0514)**

Table 5.4: Mean values of KS_{Stable} (SD shown in parenthesis)

Signals	Set A	Set B	Set C	Set D	Set E
Band-limited	0.0134 (0.0041)	0.0138 (0.0042)	0.0179 (0.0064)	0.0228 (0.0128)	0.0714 (0.0429)
IMF1	0.0171 (0.0060)	0.0242 (0.0083)	**0.0175 (0.0062)**	0.0250 (0.0200)	**0.0387 (0.0168)**
IMF2	0.0146 (0.0050)	0.0157 (0.0056)	0.0237 (0.0075)	0.0261 (0.0140)	0.0349 (0.0255)
IMF3	0.0203 (0.0075)	0.0213 (0.0067)	0.0260 (0.0077)	0.0388 (0.0980)	0.0288 (0.0130)
IMF4	0.0287 (0.0090)	0.0288 (0.0098)	0.0308 (0.0116)	0.0341 (0.0142)	0.0300 (0.0109)
IMF5	0.0415 (0.0134)	0.0452 (0.0161)	0.0462 (0.0140)	0.0461 (0.0179)	0.0467 (0.0204)
IMF6	0.0767 (0.0309)	0.0846 (0.0449)	0.0849 (0.0391)	0.0867 (0.0471)	0.0865 (0.0545)
IMF7	**0.1363 (0.0729)**	0.1287 (0.0516)	0.1393 (0.0522)	**0.1369 (0.0552)**	**0.1329 (0.0583)**
IMF8	**0.1833 (0.0531)**	**0.1928 (0.0519)**	0.2086 (0.0556)	**0.1944 (0.0538)**	**0.1807 (0.0577)**
IMF9	**0.1947 (0.0426)**	**0.2066 (0.0381)**	**0.1921 (0.0653)**	**0.1859 (0.0686)**	**0.1926 (0.0537)**

From Table 5.3 and 5.4 it can be observed that the KS measure conforms to that of KLD stating better performance of stable pdf. NIG performs better for a few types of signals (shown in bold type on the tables). The KLD measure has shown better fiiting of band-limited EEGs than the IMFs for both NIG and stable pdf, but the KS measure represents different phenomena. According to KS measure, fitting of NIG pdf is better for the first IMFs in all datasets than the band-limited EEGs. In addition to that, stable pdf is better fitted to the first IMFs for Set C and Set E than the band-limited EEGs. These two variations are shown in bold type blue color.

As a whole, we can see better statistical modeling can be achieved with original EEG signals than their empirically decomposed IMFs. Furthermore, stable pdf performs better than NIG pdf in fitting the EEG signals used in this thesis.

5.6 Summary

In this chapter, statistical modeling of EEG signals and their IMFs is investigated for NIG and stable pdfs. The goodness-of-fit is evaluated in terms KLD and KS measure. These measures indicate that stable pdf fits better than NIG pdf for all the band-limited EEGs and most of the IMFs. Moreover, both KLD and KS measures suggest better modeling of band-limited EEGs than their IMFs without a few exceptions.

Since EEG signals are statistically modeled through the estimation of parameters of a standard pdf, these parameters should be unique for each EEG signal and hence they may have the discriminating capability of EEG signals. To observe this, one-way ANOVA analysis is carried out for the estimated parameters of stable pdfs when fitted to the band-limited EEG signals.

CHAPTER 6

CONCLUSION

6.1 Summary of Research

The necessity of an automatic seizure detection system can't be neglected, considering the severity of epilepsy disease and the requirement of continuous monitoring of EEG records for proper medical treatment. Although, a number of feature based classification methods are reported in the literature, the constraint of computational complexity as well as the dimension of the feature sets are still a big issue on the way of developing more robust and efficient detection system.

In this thesis, an automated seizure detection and epilepsy diagnosis system has been proposed based on ANN and EEG features obtained in the EMD domain. Three statistical features such as variance, skewness and kurtosis, have been calculated for all the IMFs as well as the band-limited EEGs. For the same set of IMFs and EEGs, three chaotic features such as LLE, CD and ApEn are also obtained. Extensive analyses have shown that all these features can exhibit statistically significant difference among various EEGs for the first four empirically decomposed IMFs. A number of classification problems relevant to practical medical applications have been designed using these features obtained from the IMFs and band-limited EEGs. A comparative study has shown that features collected from the IMFs perform better than those obtained from band-limited EEGs in classifying the EEG segments. Furthermore, statistical features are found to have greater impact than the chaotic ones in improving the classification performance. Using the EMD domain features, the proposed methodology has been shown to achieve 100% sensitivity, 100% specificity and 100% accuracy in all the cases of classification problem with reduced computational complexity. Further investigation has been done by fitting NIG and stable pdfs to the EEG signals in an attempt to explore their underlying statistics. A quantitative analysis of goodness-of-fit has revealed that stable pdf has better fitting capability than NIG pdf and in fact the original EEG signals are better fitted than their decomposed IMFs.

6.2 Recommendations for Future Research

The EMD process used in this thesis is generally referred to *univariate* EMD. The potential of *multivariate* EMD [44] is yet to be explored in analyzing multi-channel EEG signals in the field of seizure detection. Further research is recommended in the field of statistical modeling of EEG signals, so that the estimated parameters can be robust enough in discriminating EEG segments recorded under different conditions but quite impossible to separate through visual inspection. In this thesis, moment based method has been employed to estimate statistical model parameters of EEGs. This method works well with large sample size. It is recommended to use maximum likelihood estimate (MLE) to fit EEGs of smaller length. In addition to that, the applicability of Kullback-Leibler relative entropy, which is measured, based on pdfs, should be investigated in the analysis EEGs as well as the decomposed IMFs. Finally, the methodology proposed in this thesis may be applied in the other EEG based analysis such as neo-natal seizure detection, sleep apnea detection, hypnosis detection and last but not the least, self-paced brain-computer-interfacing [45].

REFERENCES

[1] Hämäläinen, M. S., Hari, R., Ilmoniemi, R. J., Knuutila, J., and Lounasmaa, O. V., "Magnetoencephalography — theory, instrumentation, and applications to non-invasive studies of the working human brain", *Rev. Mod. Phys.*, vol. 65, No. 2, pp. 413–497, 1993.

[2] Berger, H., "Uber das Electrenkephalogramm des Menchen," *Archiv für Psychiatrie und Nervenkrankheiten*, vol. 87, pp. 527–570, 1929.

[3] Jasper, H. H., "Report of the Committee on Methods of Clinical Examination in Electroencephalography", *Electroenceph. Clin. Neurophysiol.*, vol. 10, pp. 370 – 375, 1958.

[4] Cooper, R, Osselton, J. W. and Shaw, J. C., (1969) *EEG Technology*. 2nd ed., Butterworths, London.

[5] World Health Organization, "Fact sheet on epilepsy", January, 2009, [Online]. Available: http://www.who.int/mediacentre/factsheets/fs999/en/index.html

[6] Fisher, N., Talathi, S., Cadotte, A. and Carney, P. R., "Epilepsy Detection and Monitoring", in *Quantitative EEG Analysis Methods and the Application*, chap. 6, pp. 157 – 183, Artech House Publishers, 2008.

[7] Wongse, W. C., Pardalos, P. M., Iasemidis, L. D., Shiau, D. S. and Sackellares, J. C., "Dynamical approaches and multi-quadratic integer for seizure prediction", *Journal of Optimization Methods and Software*, vol. 20, no. 2 – 3, pp. 389 – 400, Taylor & Francis Group Ltd., UK, 2005.

[8] McSharry, P. E., He, T., Smith, L. A. and Tarassenko, L., "Linear and non-linear methods for Automatic seizure detection in scalp electro-encephalogram recordings", *Journal of Med. Biol. Eng. Comput.*, vol. 40, pp. 447–461, Springer, Berlin, 2002.

[9] Gautama, T., Mandic, D. P. and Hulle, M. M. V., "Indications of nonlinear structures in brain electrical activity", *Physical Review E*, vol. 67, no. 046204, 2003.

[10] Mohseni, H. R., Maghsoudi, A. and Shamsollahi, M. B., "Seizure Detection in EEG signals: A Comparison of Different Approaches", in *Proc. of 28th Annual Intl. Conf. of IEEE EMBS*, pp. 6724 – 6727, Aug. 30 – Sept. 3, 2006.

[11] Adeli, H., Dastidar, S. G. and Dadmehr, N., "A Wavelet-Chaos Methodology for Analysis of EEGs and EEG Sub-bands to Detect Seizure and Epilepsy", *IEEE Trans. on Biomedical Engineering*, vol. 54, no. 2, pp. 205 – 211, Feb. 2007.

[12] Güler, N. F., Übeyli, E. D. and Güler, İ, "Recurrent neural networks employing Lyapunov exponents for EEG signals classification", *Elsevier Expert Systems with Applications*, vol. 29, pp. 506–514, 2005.

[13] Güler, İ. and Übeyli, E. D., "Multiclass Support Vector Machines for EEG-Signals Classification", *IEEE Transactions on Information Technology in Biomedicine*, vol. 11, no. 2, pp. 117 – 126, March, 2007.

[14] Liang, S. F., Wang, H. C., and Chang, W. L., "Combination of EEG Complexity and Spectral Analysis for Epilepsy Diagnosis and Seizure Detection", *EURASIP Journal on Advances in Signal Processing*, vol. 2010, article id. 853434, Hindawi Publishing Corporation, 2010.

[15] Schneider, M., Mustaro, P. N. and Lima, C. A. M., "Automatic Recognition of Epileptic Seizure in EEG via Support Vector Machine and dimension fractal", in *Proc. of Intl. Joint Conf. on Neural Networks*, pp. 2841 – 2845, June 14 – 19, 2009.

[16] Bedeeuzzaman M. V., Farooq O. and Khan, Y. U., "Automatic Seizure Detection Using Higher Order Moments", in *Proc. of Intl. Conf. on Recent Trends in Info., Telecomm. and Comput.*, pp. 159 – 163, March, 2010.

[17] Fathima, T., Khan, Y. U., Bedeeuzzaman, M. and Farooq, O., "Discriminant Analysis for Epileptic Seizure Detection", in *Proc. of Intl. Conf. on Devices and Communications*, Feb. 24 – 25, 2011.

[18] Tzallas, A. T., Tsipouras, M. G. and Fotiadis, D. I., "Automatic Seizure Detection Based on Time-Frequency Analysis and Artificial Neural Networks", *Computational Intelligence and Neuroscience*, vol. 2007, article id. 80510, Hindawi Publishing Corporation, 2007.

[19] Tzallas, A. T., Tsipouras, M. G. and Fotiadis, D. I., "Epileptic Seizure Detection in EEGs Using Time–Frequency Analysis", *IEEE Transactions on Information Technology in Biomedicine*, vol. 13, no. 5, pp. 703 – 710, Sept. 2009.

[20] Pachori, R. B., "Discrimination between Ictal and Seizure-Free EEG Signals Using Empirical Mode Decomposition", in *Research Letters in Signal Processing*, vol. 2008, article id. 293056, Hindawi Publishing Corporation, 2008.

[21] Orosco, L., Laciar, E., Correa, A. G., Torres A. and Graffigna, J. P., "An Epileptic Seizures Detection Algorithm based on the Empirical Mode Decomposition of EEG", in *Proc. of 31st IEEE EMBS Annual Intl. Conf.*, pp. 2651 – 2654, Sept. 2 – 6, 2009.

[22] Orosco, L., Correa, A. G. and Laciar, E., "Multiparametric Detection of Epileptic Seizures using Empirical Mode Decomposition of EEG Records", in *Proc. of 32nd IEEE EMBS Annual Intl. Conf.*, pp. 951 – 954, Aug. 31 – Sept. 4, 2010.

[23] Alam, S M S. and Bhuiyan, M. I. H., "Detection of Epileptic Seizures using Higher-order Statistics in the EMD Domain", (*submitted*), *Journal of Med. Biol. Eng. Comput.*,Springer, Berlin.

[24] Huang, N. E., Shen, Z., Long, S. R., Wu, M. C., Shih, H. H., Zheng, Q., Yen, N. C., Tung, C. C., and Liu, H. H., "The empirical mode decomposition and the Hilbert spectrum for nonlinear and non- stationary time series analysis", in *Proc. of R. Soc. London, Ser. A*, vol. 454, no. 1971, pp. 903–995, 1998.

[25] EEG time series download page. [Online]. Available: http://epileptologie-bonn.de/cms/front_content.php

[26] Ralph G. Andrzejak, R. G., Lehnertz, K., Mormann, F., Rieke, C., David, P., and Elger, C. E., "Indications of nonlinear deterministic and finite-dimensional structures in time series of brain electrical activity: Dependence on recording region and brain state", *Phys. Rev. E*, vol. 64, no. 6, pp. 1 – 8, 2001.

[27] Vogl, T. P., Mangis, J. K., Rigler, A. K., Zink, W. T. and Alkon, D. L., "Accelerating the convergence of the backpropagation method," *Biological Cybernetics*, vol. 59, pp. 257 – 263, 1988.

[28] Møller, M. F., "A scaled conjugate gradient algorithm for fast supervised learning," *Neural Networks*, vol. 6, no. 4, pp. 525 – 533, 1993.

[29] Alam, S M S., Bhuiyan, M. I. H., Aurangozeb and Shahriar, S. T., "EEG Signal Discrimination using Non-linear Dynamics in the EMD Domain", in *Proc. of 3rd Intl. Conf. on Signal Acquisition and Processing*, vol. 1, pp. 231 – 235, Feb. 26 – 28, 2011.

[30] Takens, F., "Detecting strange attractors in turbulence", *Dynamical Systems and Turbulence, Lecture notes in Math.*, vol. 898, pp. 366 – 381, Springer-Verlag, Heidelburg, 1981.

[31] Cao, L., "Practical method for determining the minimum embedding dimension of a scalar time series," *Physica D: Nonlinear Phenomena*, vol. 110, no. 1–2, pp. 43–50, 1997.

[32] Wolf, A., Swift, J. B., Swinney H. L. And Vastano, J. A., "Determining Lyapunov Exponents from a time series", *Physica D: Nonlinear Phenomena*, vol. 16, no. 3, pp. 285 – 317, 1985.

[33] Parlitz, U., "NONLINEAR TIME SERIES ANALYSIS", in J. A. K. Suykens and J. Vandewalle (eds.). *Nonlinear Modelling–Advanced Black-box Techniques*, chap. 8, pp. 209 – 239, Kluwer Academic Publishers, Boston, 1998.

[34] Grassberger, P. and Procaccia, I., "Characterization of strange attractors", *Phys. Rev. Lett.*, vol. 50, no. 5, pp. 346 – 349, January, 1983.

[35] Takens, F., "Numerical determination of the dimension of an attractor", *Dynamical Systems and bifurcations, Lecture notes in Math.*, vol. 1125, pp. 99 – 106, Springer, Berlin, 1985.

[36] Alam, S M S. And Bhuiyan, M. I. H., "Detection of Epileptic Seizures using Chaotic and Statistical Features in the EMD Domain", (*submitted*), *2011 Annual IEEE India Conference* (*IEEE INDICON 2011*).

[37] Pincus, S. M., "Approximate entropy as a measure of system complexity", in *Proc Natl. Acad. Sci. USA*, vol. 88, pp. 2297 – 2301, 1991.

[38] Natarajan, K., Acharya, R. U., Alias, F., Tiboleng, T., and Puthusserypady, S. K., "Nonlinear analysis of EEG signals at different mental states", *Bio Medical Engineering On Line*, vol. 3, no. 7, 2004.

[39] Hanssen, A. and Øigård, T. A., "The normal inverse Gaussian distribution for heavy-tailed processes," in *Proc. IEEE-EUEASIP Workshop on Nonlinear Signal and Image processing*, 2001.

[40] Nolan, J. P., "Basic Properties of Univariate Stable Distributions", in *Stable Distributions-Models for Heavy Tailed Data*, chap 1, pp. 3 – 24, 2009.

[41] STBL toolbox. [Online]. Available: http://math.bu.edu/people/mveillet/research.html

[42] Bhuiyan, M. I. H., Ahmad, M. O. and Swamy, M. N. S., "Modeling of the DCT Coefficients of Images", in *Proc. of IEEE International Symposium on Circuits and Systems*, pp. 272 – 275, 2008.

[43] Press, W. H., Teukolsky, S. A., Vellerling, W. T. and Flannery, B. P. (1999) *Numerical Recipes in C: The Art of Scientific Computing*. Cambridge University Press, UK.

[44] Rehman, N. and Mandic, D. P., "Multivariate empirical mode decomposition", *Proc. R. Soc.*, vol. 466, pp. 1291–1302, 2010.

[45] Rao, R. P. N. and Scherer, R., "Brain-Computer Interfacing", *IEEE Signal Processing Magazine*, pp. 152, 148 – 150, July, 2010.